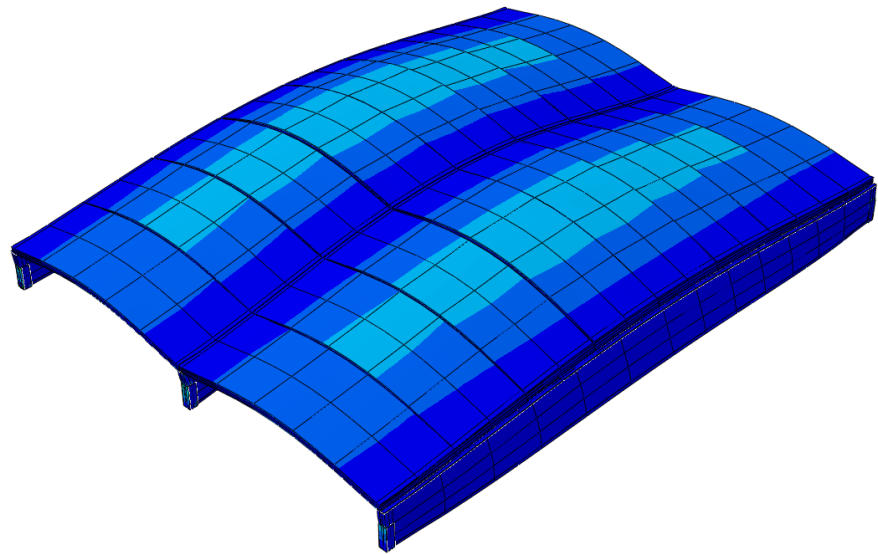




LUND
UNIVERSITY



DESIGN OF A GLASS FLOOR STRUCTURE

PONTUS DUFVENBERG and FREDRIK JÖNSSON

Structural
Mechanics

Master's Dissertation

DEPARTMENT OF CONSTRUCTION SCIENCES
DIVISION OF STRUCTURAL MECHANICS

ISRN LUTVDG/TVSM--14/5192--SE (1-65) | ISSN 0281-6679

MASTER'S DISSERTATION

DESIGN OF A GLASS FLOOR STRUCTURE

PONTUS DUFVENBERG and FREDRIK JÖNSSON

Supervisor: **PER-ERIK AUSTRELL**, Assoc. Professor; Div. of Structural Mechanics, LTH, Lund.

Examiner: **KENT PERSSON**, PhD; Div. of Structural Engineering, LTH, Lund.

Copyright © 2014 Division of Structural Mechanics
Faculty of Engineering (LTH), Lund University, Sweden.

Printed by Media-Tryck LU, Lund, Sweden, March 2014 (*PI*).

For information, address:

Div. of Structural Mechanics, LTH, Lund University, Box 118, SE-221 00 Lund, Sweden.

Homepage: <http://www.byggmek.lth.se>

Preface

The work presented in this master thesis was carried out at The Division of Structural Mechanics, Department of Construction Sciences, Lund University. This report is the end stage of several years of studies at The Faculty of Engineering (LTH) at Lund University, which finally ends up in a Master's Degree in Civil Engineering.

We would like to express our gratitude to Kent Persson for sharing his knowledge concerning finite element modelling and the behaviour of glass structures. Thank you for always having the door open and taking your time helping us.

During our time at the Department of Construction Sciences there has never been a problem for us to ask questions and get advice from anyone of the staff. We are sincerely grateful to have had this opportunity and to be a part of the interesting coffee breaks and meetings at the institution.

Our time at the university has been an interesting journey and the years passed in Lund are never to be forgotten. We would like to thank friends we gained during our time here, without you this journey would never have been the same. Special thanks to Martin Andersson and Mark Bellingham for proofreading this report.

Finally we would like to thank our families for all your support throughout our education.

Lund, March 2014

Pontus Dufvenberg and Fredrik Jönsson

Abstract

Glass is by procurers and architects regarded as a material with desirable aesthetic properties and is therefore more frequently utilized as a building material. A problem though, is that glass is a brittle material sensitive to stress concentrations and imperfections. Knowledge about glass as a bearing structural element is limited, but is steadily improving. The aim of this report was to design a load bearing structure consisting of a glass floor supported by glass beams. The analyses were carried out using heat strengthened glass layers with SentryGlasPlus as laminating interlayers.

Analyses of the system were mainly carried out using the finite element software Abaqus CAE. Different cross sections of glass plates were analysed with the purpose to determine stresses and deflections in the profiles. Cracks were introduced to the plates and the influence of these was investigated with approximate analytical calculations and reference work. A laminated glass plate consisting of two 12 mm glass layers in the centre and two 8 mm glass layers outermost was considered acceptable when carrying a uniformly distributed load on a simply supported glass plate of length 1.5 m. The glass profile was considered adequate both for a cracked and an uncracked profile.

The beams were analysed using static- and buckling analyses in Abaqus. When the static analyses were performed, both a cracked and an uncracked profile were tested. Distributions of the cracks were determined with a previously performed test study and calculations performed in Abaqus. Stresses, strains and deflections were determined in the cross section to validate the chosen profile. A reinforcing steel bar was decided to act in the bottom of the beam to prevent a hasty breakage if the glass would start to crack. A beam consisting of three laminated glass layers with a thickness of 15 mm each was decided as the cross section. A quadratic bar of $15 \times 15 \text{ mm}^2$ steel reinforcement was decided to act in the bottom of the centric glass layer. The total height of the beam was chosen to be 250 mm and the total length was 4 m.

Analyses were carried out concerning vibrations using a combined structure of beams and plates. The response of both vertical and lateral vibrations was investigated concerning the system. The calculated vibrations were below the allowed limits.

A simplified calculation of the system's resistance against fire was performed and a few suggestions concerning actions to construct a resistant glass system is presented.

Finally a discussion concerning the entire report and suggestions for further work are presented.

Sammanfattning

Glas är av arkitekter och beställare ansett som ett material med tillfredställande estetiska egenskaper och används därför allt mer frekvent som byggnadsmaterial. Ett problem är dock det faktum att glas är ett sprött material, känsligt för spänningskoncentrationer och imperfektioner. Kunskapen om glas som bärande element är begränsad, men är under ständig utveckling. Syftet med denna rapport var att dimensionera ett glasgolv uppbyggt av glasbalkar. Värmeförstärkta glasskikt användes med SentryGlasPlus som laminat mellan glasskivorna.

Analyserna utfördes främst med hjälp av programvaran Abaqus CAE. Olika tvärsnitt av glasplattor analyserades med syfte att bestämma spänningar och förskjutningar i profilerna. Sprickor introducerades även i plattorna och dess påverkan utvärderades genom approximativa analytiska beräkningar och referensarbeten. En laminerad glasplatta bestående av två 12 mm glasskikt centralt och två 8 mm glasskikt ytterst ansågs tillräckligt gällande bärförmåga av en jämt utbredd last på en 1.5 m lång fritt upplagd platta. Profilen ansågs tillräcklig gällande både ett sprucket och ett intakt tvärsnitt.

Balkarna analyserades med en statisk analys, samt med en instabilitetsanalys i Abaqus. När den statiska analysen genomfördes studerades både en sprucken och en intakt profil. Sprickornas utbredning bestämdes genom en jämförelse med tidigare genomförd studie, samt beräkningar i Abaqus. Spänningar, töjningar och nedböjning bestämdes i tvärsnittet för att tillgodose en tillräcklig profil för syftet. Ett armeringsband tillverkat av stål bestämdes verka i botten av balken för att förebygga ett sprött brott om sprickbildning i glaset skulle uppstå. En balk innehållande tre laminerade glasskikt med en tjocklek på 15 mm vardera bestämdes verka tillsammans i tvärsnittet. Ett kvadratisk $15 \times 15 \text{ mm}^2$ armeringsband av stål valdes verka i botten av det centriska glasskiktet. Balkens totala höjd sattes till 250 mm och den totala längden till 4 m.

En analys gällande vibrationer i ett kombinerat system av balkar och plattor genomfördes och responsen av både vertikala och horisontala vibrationer i systemet utvärderades. Beräknade vibrationer visade sig vara under givna riktvärden.

En förenklad beräkning genomfördes gällande systemets motståndskraft mot brand och några åtgärder beträffande uppförandet av ett brandmotståndskraftigt system presenterades.

Slutligen fördes en diskussion gällande hela rapporten där rekommendationer för fortsatta studier presenterades.

Contents

1	Introduction	1
1.1	Background.....	1
1.2	Objective and method.....	1
1.3	Disposition.....	2
2	Description of the glass system	3
2.1	Intended system.....	3
2.2	Reference work.....	3
3	Materials	7
3.1	Glass.....	7
3.1.1	Annealed glass.....	8
3.1.2	Heat strengthened glass.....	8
3.1.3	Tempered glass.....	8
3.1.4	Comparison and choice of glass material.....	8
3.2	Polymer interlayer.....	8
3.3	Rubber.....	9
3.4	Adhesive.....	10
3.5	Steel.....	10
4	Theory	11
4.1	The Finite element method.....	11
4.1.1	Introduction.....	11
4.1.2	Modelling of linear-elastic materials.....	11
4.1.3	Equation of motion.....	12
4.1.4	Finite elements.....	12
4.1.5	Isoparametric finite elements.....	12
4.2	Structural dynamics.....	13
4.2.1	Springs.....	13
4.2.2	Modelling rubber boundaries.....	13
4.2.3	Steady state.....	13
4.2.4	Damping.....	14
4.2.5	Rayleigh damping.....	15
4.3	Buckling analysis.....	16
4.4	Abaqus modelling.....	16
5	Eurocode and standards	17
5.1	Design value of strength for heat strengthened glass.....	17
5.2	Design of the glass structure.....	18
5.2.1	Design value for loading in ultimate limit state.....	18
5.2.2	Serviceability limit state.....	18
5.3	Vibration analysis.....	19
6	Design of glass plates	21
6.1	Estimation of a glass plate.....	21
6.1.1	Conclusion considering shear force.....	22
6.2	Analysis of stresses and deflections.....	22
6.2.1	Abaqus modelling.....	22
6.2.2	Meshing of the glass plates.....	23
6.2.3	Description of the analysis.....	24
6.3	Results from the static analyses.....	26
6.3.1	Conclusion static analysis.....	27

6.4	Cracked glass plates.....	28
6.5	Analytically calculated strength of cracked glass plates	29
6.6	Conclusions and choice of glass plates.....	32
7	Design of glass beams	33
7.1	Estimation of a glass beam	33
7.1.1	Conclusion considering shear force	33
7.2	Analysis of stresses, strains and deflections	33
7.2.1	Abaqus modelling	33
7.2.2	Description of the analysis	34
7.2.3	Modelling of the cracks in the beam	35
7.2.4	Modelling of multiple cracks in the beam.....	37
7.3	Analysis of buckling	38
7.3.1	Abaqus modelling	38
7.3.2	Description of the buckling analysis	39
7.4	Results.....	42
7.4.1	Static analysis.....	42
7.4.2	Buckling analysis	43
7.5	Modelling of beams presented from previous study.....	43
7.5.1	Description of the analysis	43
7.5.2	Results	44
7.6	Conclusions.....	45
8	Vibration analysis	47
8.1	Analysis of the system	47
8.1.1	Abaqus modelling	47
8.1.2	Evaluation of vibrations	48
8.2	Results.....	50
8.2.1	Damping coefficients	50
8.2.2	Vibrations.....	50
8.3	Conclusions of the vibration analysis	52
9	Design of the whole system involving boundaries	53
9.1	Description of the system with dimensions	53
9.2	Wear layer.....	54
9.3	Attachments	54
9.4	Erection of the system	54
10	Design concerning resistance against fire	57
10.1	Fire progression	57
10.2	Fire safety requirements	57
10.3	Fire resistance of glass.....	58
10.4	Fire resistance of polymers.....	58
10.5	Simulation of fire.....	58
10.6	Conclusion	60
11	Final remarks	61
11.1	Conclusions	61
11.2	Further studies	61
12	Bibliography	63

1 Introduction

1.1 Background

The usage of glass as a structural element is common around the globe today; it is regarded as a material with desirable aesthetical properties by procurers and architects. Technological developments have made it possible to have glass elements with relatively slender profiles as the main bearing system. The problem though is that glass is a brittle material sensitive to stress concentrations at supports and to imperfections, such as micro-cracks. This makes glass a quite unreliable material concerning safety and breakage. The usage of polymer interlayers makes it possible to hold several glass layers together even if cracks would occur and it reduces the risk for cracking to spread between the laminated sections.

To imagine a bearing structure containing a glass floor carried by slender glass beams is a fascinating idea, which as far as the authors are aware, has never been carried out. Several similar solutions have been managed on the other hand, such as the Apple glass cube in New York. In this structure, a glass beam frame carries a box of glass which is the entrance to one of the Apple stores in the city. In other examples glass is used in stairways, or as a floor which is the case of the Grand Canyon Skywalk.

1.2 Objective and method

The aim of this master's dissertation is to design a load bearing structure consisting of a glass floor supported by glass beams. Supports will also be considered. The dimensions of the glass structure members with attachments will be determined with calculations performed with the software Abaqus.

Analysis will be carried out concerning static loading and buckling of the beams. Evaluations will be made for dynamic loads acting on the system.

The calculations concerning the beams in this report will be confirmed by an analysis in Abaqus of reinforced glass beams that have previously been tested in a laboratory study carried out by [5].

1.3 Disposition

The report includes the following chapters:

- In Chapter 2 the intended glass system is described.
- In Chapter 3 the materials glass, polymer interlayer, rubber, adhesive and steel are generally described.
- In Chapter 4 the finite element method is generally described and structural dynamics theory is introduced as well as vibration and buckling theory.
- In Chapter 5 Eurocode and standards are presented.
- In Chapter 6 the design of the glass plates with results is presented.
- In Chapter 7 the design of the glass beams with results is presented. An analysis regarding the tests carried out by [5] is also presented as verification.
- In Chapter 8 a study of the glass system concerning vibrations is carried out.
- In Chapter 9 the whole system is presented with connections.
- In Chapter 10 the system's resistance to fire is discussed.
- In Chapter 11 final remarks and suggestions for further work are presented.

2 Description of the glass system

In this chapter a brief description of the indented glass system is given with some references to a previously performed study.

2.1 Intended system

The system contains a glass floor supported by glass beams, in this case carried by steel columns. All beams and plates are simply supported. The intended structure can be seen in Figure 2.1.

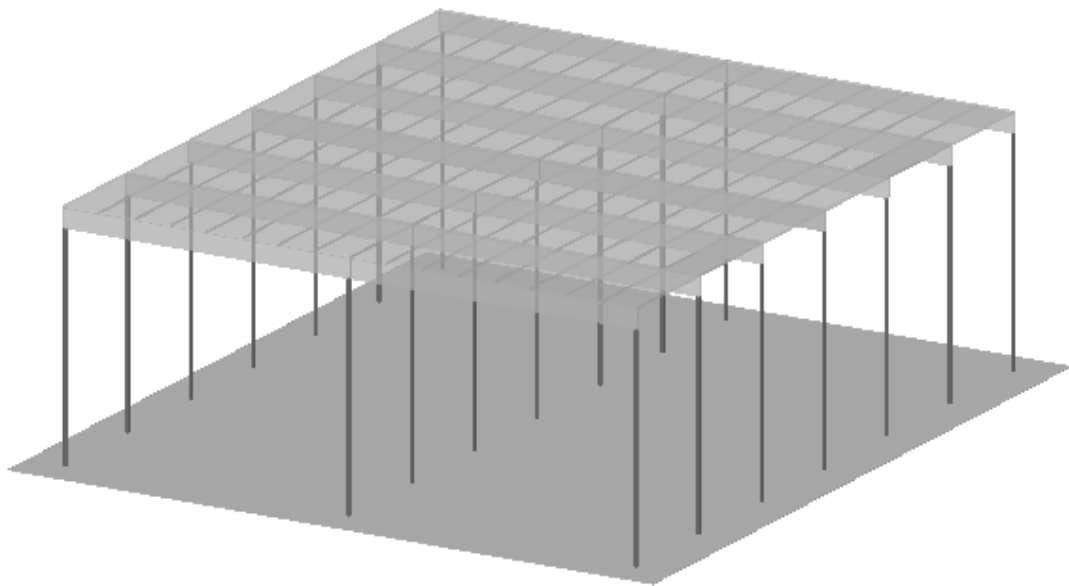


Figure 2.1: Sketch of the intended structure.

The beams that were investigated in the work presented in this report were decided to have a span of 4 m and a spacing of 1.5 m between each other. The beams are simply supported with boundaries based on steel columns. Each meter of a beam carries a load of 1.5 m glass plate. The glass plates have a dimension of 0.5x1.5 m each and are connected to the beams with a silicone adhesive and spacers made of EPDM-rubber. Silicone is also used in the connection between all plates. The beams are attached to the steel columns with U-formed boundaries made out of steel with the inside covered with rubber. A rubber cover is also placed in the connection between every simply supported beam at the boundary on the columns.

2.2 Reference work

The report described in [5] presents tests concerning three different beams, all built up from three glass layers laminated together with a steel reinforcement in the bottom of the mid-layer. The dimensions of a single beam are presented in Figure 2.2.

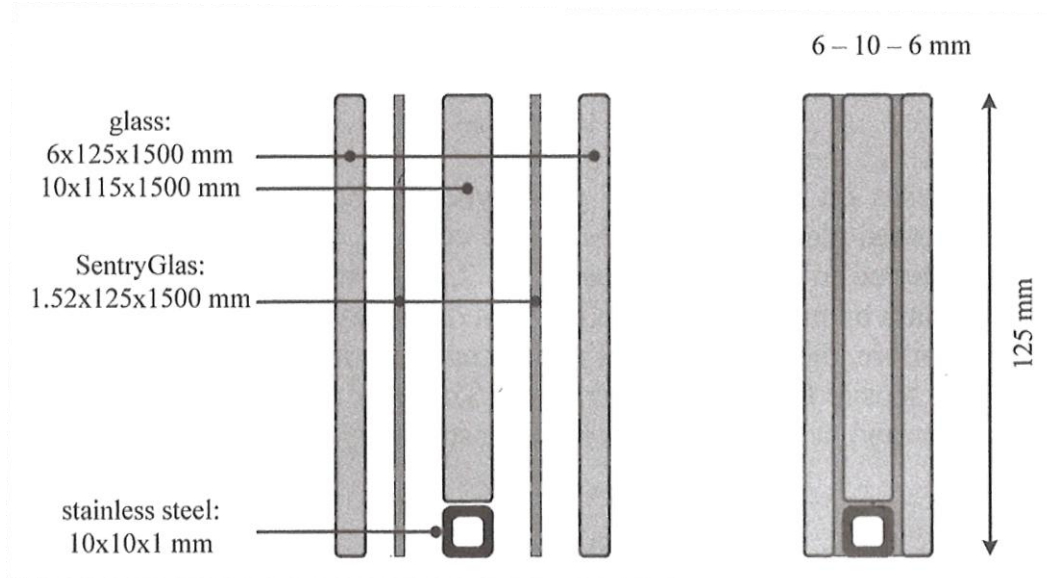


Figure 2.2: Dimensions of the reference work beam [5].

The beam shown in Figure 2.2 has several benefits which are stated below:

- Glass is a brittle material and therefore sensitive to cracking. By using a plastic material in between and laminate several layers of glass together, it enables a profile that is still capable to carry load even if cracking has occurred.
- Flat thin profiles are desirable in the manufacturing process. It is easier to make them affordable and to control the quality of the material.
- This kind of profile enables a bar of steel reinforcement to be easily installed in the centre at the bottom of the cross section. The purpose of the reinforcement is to take the tensile stresses if cracking occurs.

The strength of the beams in [5] was investigated for three choices of glass types. The beams tested consisted of annealed glass, heat strengthened glass and fully tempered glass. Each beam had a support span of 1400 mm and was subjected to a four point bending test as can be seen in Figure 2.3. The study showed that fully tempered glass gives the best results concerning the initial breakage load, since it was capable of taking the highest load. Heat strengthened glass on the other hand showed a better result concerning the maximum post breakage load.

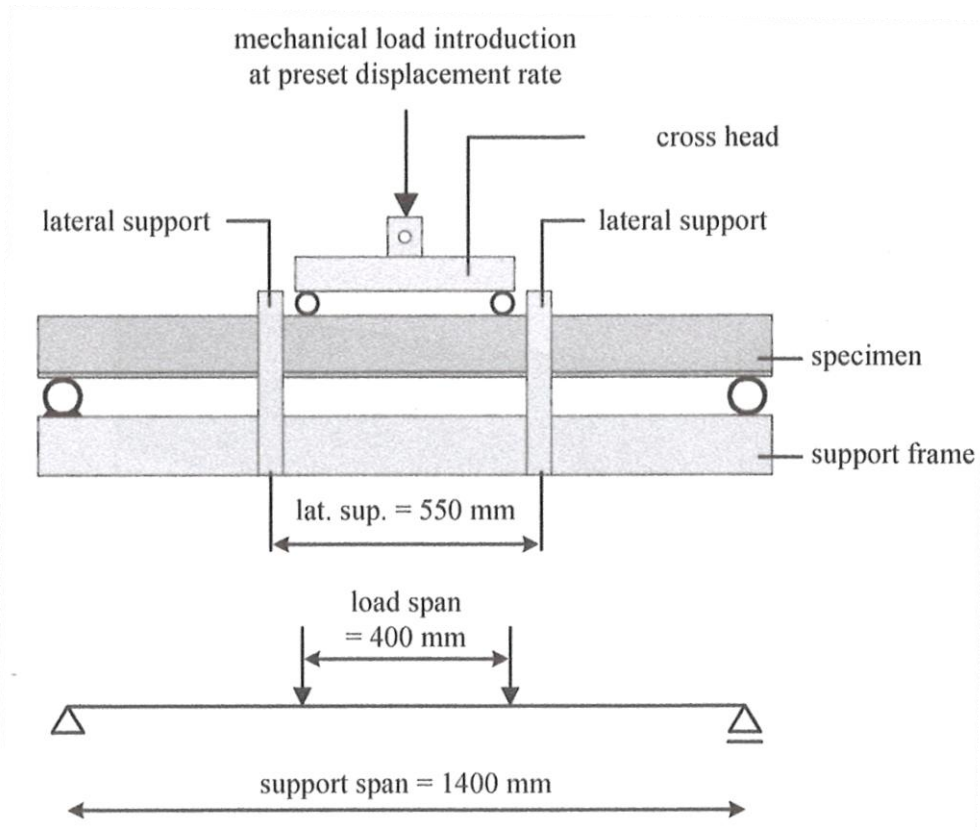


Figure 2.3: Reference work four-point bending test setup [5].

The results concerning the beams are interesting in the verification of the theoretical calculations carried out in this report. In Section 7.6 a comparison with the result from [5] and a model made in Abaqus will be performed.

3 Materials

When glass is used as a material in plates, different options are possible. One possibility is to use a single solid piece of glass. Another option is to put several layers of smaller glass plates together with plastic layers in between. This procedure is called lamination and the product is known as a laminated plate.

Glass is a material with a brittle behaviour. When glass is critically loaded, micro cracks which exist in the material will instantly grow resulting in total breakage of the glass profile. This kind of failure happens instantly as the required amount of fracture energy is low. Typical for the failure surfaces is that they will not deform during the process [31].

Concerning a beam element, glass can be used as a solid. However, the development of cracks and the difficulties for the manufacturer to make a profile big enough are problems to be solved. If the glass is laminated in a few layers it will result in a more ductile and reliable cross section, which also is easier to fabricate. Glass is a high strength material for compression loading but not as good when considering tensile loading. This is due to the micro cracks in the surface which will weaken the material considerably [1].

When the strength of a glass material is exceeded, continuous cracks will develop fast in the material if a tensile state is present. Therefore it is necessary to have some kind of safety built in to prevent fast brittle breakage. In this report, the safety added is a steel bar of reinforcement in the bottom of the beams where tensile stresses act. If a crack occurs, the reinforcement will take the tensile stresses and prevent a sudden failure of the structure.

3.1 Glass

Glass is a non-crystalline product produced by sand and alkalis fused together [1]. Glass has a plastic behaviour in the molten state, soft and malleable when hot and brittle when it is cold. Normal room temperature is considered cold; hence glass has a brittle behaviour.

Fracturing in a glass section occurs at much lower stresses when the specimen is loaded in tension than when it is loaded in compression. The theoretical compressive strength of glass can be as high as 16 GPa [23], however this value is well above experimental values.

Melting is the central phase in glass manufacturing [1]. The individual raw materials react and combine in high temperatures around 1400°C. The glass is then cooled down to a lower temperature where it is shaped to the desirable form. After shaping, the material must be cooled, initially at a temperature just below where the glass begins to soften (450-550 °C). The temperature is then slowly lowered until room temperature is reached to remove residual stresses inside the glass. If the cooling is carried out too quickly, tension will remain inside the glass cross section. This will result in stresses built into the section, which may cause cracking. However if the

temperature is slowly lowered to the cold state in a correct way, no stresses will remain inside the cross section.

Sometimes stresses are desirable in a glass plate. For structural design purposes, tension inside a glass plate and compression at the surface means that the plate can take much higher loads [2]; this is called a heat-treated glass. The mechanical strength of heat-treated glass varies significantly depending on the glass surface condition. This is also the case concerning cracking behaviour. Glass can be divided into several groups depending on the fabrication process. In this report three groups are of interest: Annealed glass, Heat strengthened glass and Tempered glass.

3.1.1 Annealed glass

Annealed glass is raw glass with low residual stresses [2]. The fracture behaviour of annealed glass profiles is a few long continuous cracks which will not expand with a chain reaction over the surface. This enables cutting of a profile during production.

3.1.2 Heat strengthened glass

Glass that has been heat-treated to have a surface compression of 70 MPa is called heat strengthened glass [20]. It has a fracture behaviour similar to annealed glass.

3.1.3 Tempered glass

Glass that has been heat-treated to have a surface compression of 120 MPa is called a tempered glass [20]. This type of glass is about three times stronger than annealed glass and breaks into small pieces at failure. This means that the entire profile most likely shatters when a single crack occurs [2].

3.1.4 Comparison and choice of glass material

Normally annealed glass is used in laminated plates, as the breakage of the glass in failure into big sharp pieces is ideal for the laminate. In comparison tempered glass breaks into small pieces the size of gravel, which is harder for the laminate interlayer to hold together [4]. The choice of glass type in laminated glass is, however, dependant of the application. Heat strengthened glass works in the span between the two other mentioned types and is possible to fabricate with a behaviour near annealed glass considering cracking. A test carried out by [3] shows that heat strengthened glass is favourable in lamination of plates, compared with tempered glass.

The fact that heat strengthened glass is about two times stronger than annealed glass and has fracture behaviour similar to annealed glass [4], leads to the conclusion that this will be the glass to be used for the design in this report. Glass normally has a density of 2500 kg/m^3 , a Poisson's ratio of 0.22 and a Young's modulus of 70 GPa [5].

3.2 Polymer interlayer

A polymer can be synthetic or natural, and consists of chain-shaped molecules [6]. All the parts in the chain-shaped molecules are bound with covalent bindings. Polymers are usually viscoelastic and will exhibit creep strains when loaded.

The glass layers considered in this report are laminated together using polymer interlayers. If the glass cracks it can still carry compressive forces; the interlayers will

help to keep the glass in its place and still allow it to be a bearing element in the structure. The glass sheets will be laminated together using SentryGlasPlus (SGP) interlayers from DuPont [7]. These interlayers are considered 5 times tougher and up to 100 times stiffer than conventional interlayer materials like PVB. The interlayers can thus carry more load and contribute more as a bearing element than other conventional materials.

SGP has a mass density of 950 kg/m^3 [7]. The stiffness and Poisson's ratio of the polymers varies with temperature and duration of the loading. For a long lasting load of 10 years with a temperature of 24°C , SGP has a stiffness of 129 MPa and a Poisson's ratio of 0.489. These material parameters will be used in the calculations of an uncracked beam with long term loading scenarios. For a short lasting load of 1 minute and a temperature of 24°C , SGP has a stiffness of 505 MPa and a Poisson's ratio of 0.458. These material parameters will be used both in the calculations of a cracked beam and in the dynamic analysis where short term loads are acting. The plastic yield stress of SGP is 23 MPa and the breaking strength is about 34.5 MPa [22].

The stress strain relation concerning SGP can be seen in Figure 3.1 [17].

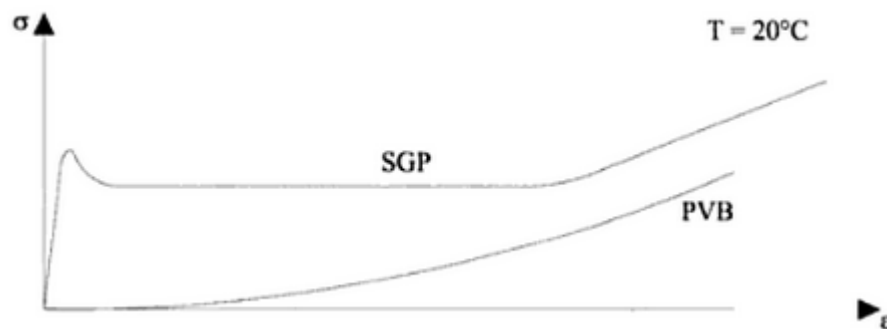


Figure 3.1: Stress-strain relation curve for SGP [17].

3.3 Rubber

Rubber is a special group of polymeric materials [8]. There are natural rubbers that are created by nature and synthetic rubbers that are manmade. Rubber is characterized by a process called vulcanization. When it undergoes vulcanization it switches to an elastic state. During the vulcanization sulphur is added and cross links are created between the molecule-chains so that a network is formed. This network gives rubber its very high elastic characteristics; the sparse network structure can be deformed when loaded and regain its original shape when unloaded [8]. An important property of a rubber component is the possibility to modify its stiffness. The stiffness of a component can be modified when the rubber is created by adding fillers or afterwards by changing the thickness of the rubber.

The boundaries of the beams will be covered with EPDM-rubber, and the spacers between the glass beams and the glass plates will be made of EPDM-rubber. This type of rubber is very resistant to aging and external aggressive conditions including

severe temperature changes [9]. Hence, the material is widely used in the construction industry and therefore assumed to be reliable.

The rubber that will be used in this report has a density of 1300 kg/m^3 , a Poisson's ratio of 0.49 and a Young's modulus of 70 GPa according to [9]. The material can take 8 MPa in tension and 400 % in elongation.

3.4 Adhesive

An adhesive is a substance that binds two objects together. The connection is accomplished by adhesion between the adhesive and the object's boundary surfaces and through cohesion in the glue joint [10]. It is required that the adhesive has low viscosity when applied and that the surface of the object has good wetting against the adhesive so that it can spread across the surface.

Glass is a brittle material which makes it sensitive to stress concentrations. Therefore adhesives are good alternatives to mechanical glass joints since it spreads the stresses over the surface of the joint. In the work presented in this report a silicone adhesive is used to join the glass beams and the glass plates. Silicone has good durability and resistance to weather, temperature, age and ultraviolet light [11]. As silicone is a soft material, spacers made out of EPDM-rubber are placed in the boundary between the glass beams and the glass plates to stiffen the connection.

3.5 Steel

Steel is the term for materials with elemental iron as the main constituent. Steel as a metal is composed of crystals having a regular array of nuclei [8]. Various types of processed steel with different kinds of properties are possible to manufacture from the molten state, most of them are isotropic materials which means that they have the same behaviour in all directions. At normal room temperature low-grade steel has ductile failure behaviour. The material will behave elastically until the upper yield stress point and will thereafter act plastically until breakage. Steel is said to have the same strength both in tensile loading as in compressive loading.

In this case austenitic stainless steel will be used as reinforcement inside the glass beams, as the corrosion risk might be high. This kind of steel has a density of 7950 kg/m^3 , a Poisson's ratio of 0.2 and a Young's modulus of 203 GPa according to [12]. Steel can be produced with a strength reaching over 1000 MPa depending on the hardening process and the choice of alloy.

4 Theory

In this chapter theoretical backgrounds to the calculations which are performed in later chapters are given. References to further reading are also suggested. An introduction to the Finite element method, structural dynamics- and vibrations theory, as well as the theory behind eigenfrequency analysis and buckling analysis is given.

4.1 The Finite element method

In this section an introduction to the theory of the finite element analysis is given. For further reading about the method see [14].

4.1.1 Introduction

The Finite element method solves differential equations in an approximate manner using a numerical approach. It is used for solving engineering problems that are too complicated to solve analytically.

Consider a variable that has an arbitrary variation over a region, then it is a good approximation to assume that it varies in a linear manner for small elements in this region. This is the basis of the Finite element method, to divide regions into smaller elements and then solve the problem approximately for each element. A region with elements is called a finite element mesh. With a finer element mesh the solution converges towards the exact solution [14].

Calculating deflections and forces with the finite element analysis is done by solving the following equation system

$$\mathbf{K}\mathbf{a} = \mathbf{f} \quad (4.1)$$

where \mathbf{K} is the stiffness matrix, \mathbf{a} is the displacements and \mathbf{f} is the forces.

4.1.2 Modelling of linear-elastic materials

The following text is a summary of the finite element formulation of a linear-elastic material, for a more extensive derivation see pages 235-260 in [14]. Theory for large deformations can be found in [25].

The relation between stresses and strains is called a constitutive relation. The simplest constitutive relation is linear elasticity expressed by Hooke's law in one dimension by eq. (4.2)

$$\sigma = E\varepsilon \quad (4.2)$$

where σ is the stress, E is Young's modulus and ε is the strain [14]. This relation also holds when there are several stress and strain components. In three dimensions the generalized Hooke's law describes the stresses and strains given by [14] as

$$\boldsymbol{\sigma} = \mathbf{D}\boldsymbol{\varepsilon} \quad (4.3)$$

where

$$\boldsymbol{\sigma} = \begin{bmatrix} \sigma_{xx} \\ \sigma_{yy} \\ \sigma_{zz} \\ \sigma_{xy} \\ \sigma_{xz} \\ \sigma_{yz} \end{bmatrix} \quad \boldsymbol{\varepsilon} = \begin{bmatrix} \varepsilon_{xx} \\ \varepsilon_{yy} \\ \varepsilon_{zz} \\ \varepsilon_{xy} \\ \varepsilon_{xz} \\ \varepsilon_{yz} \end{bmatrix} \quad (4.4)$$

and

$$\mathbf{D} = \frac{E}{(1+\nu)(1-2\nu)} \begin{bmatrix} 1-\nu & \nu & \nu & 0 & 0 & 0 \\ \nu & 1-\nu & \nu & 0 & 0 & 0 \\ \nu & \nu & 1-\nu & 0 & 0 & 0 \\ 0 & 0 & 0 & \frac{1}{2}(1-2\nu) & 0 & 0 \\ 0 & 0 & 0 & 0 & \frac{1}{2}(1-2\nu) & 0 \\ 0 & 0 & 0 & 0 & 0 & \frac{1}{2}(1-2\nu) \end{bmatrix} \quad (4.5)$$

In modelling of plasticity concerning the material, theory is to be found in [26].

4.1.3 Equation of motion

The linear dynamic FE-formulation of an undamped MDOF-system is given by [16] as

$$\mathbf{M}\ddot{\mathbf{a}} + \mathbf{K}\mathbf{a} = \mathbf{f} \quad (4.6)$$

where \mathbf{M} is mass matrix, $\ddot{\mathbf{a}}$ is the accelerations, \mathbf{K} is the stiffness matrix, \mathbf{a} is the displacements and \mathbf{f} is the load vector.

4.1.4 Finite elements

The elements used in the FE-calculations are three dimensional deformable solids. Assuming that the displacements vary in a quadratic manner in the elements the geometric order is chosen to be quadratic. The solid elements are thus 20 node brick elements.

4.1.5 Isoparametric finite elements

For a brick element to behave in a compatible manner the sides of the element must be parallel to the coordinate axes. This leads to restrictions concerning modelling of bodies with arbitrary geometry. However, with the use of isoparametric finite elements it is possible to establish compatible finite elements that have curved boundaries [14].

This is achieved by mapping of one region into another region. The region that contains the arbitrary geometry is called the global domain and the region containing a square geometry is called the parent domain. For three dimensional finite elements the parent domain is a cube bound by the lines $\xi=\pm 1$, $\eta=\pm 1$ and $\zeta=\pm 1$ according to Figure 4.1. This mapping is given by [14] as

$$x = x(\xi, \eta, \zeta); \quad y = y(\xi, \eta, \zeta); \quad z = z(\xi, \eta, \zeta) \quad (4.7)$$

The mapping results in that every point in the parent domain has a corresponding point in the global domain which can be seen in Figure 4.1.

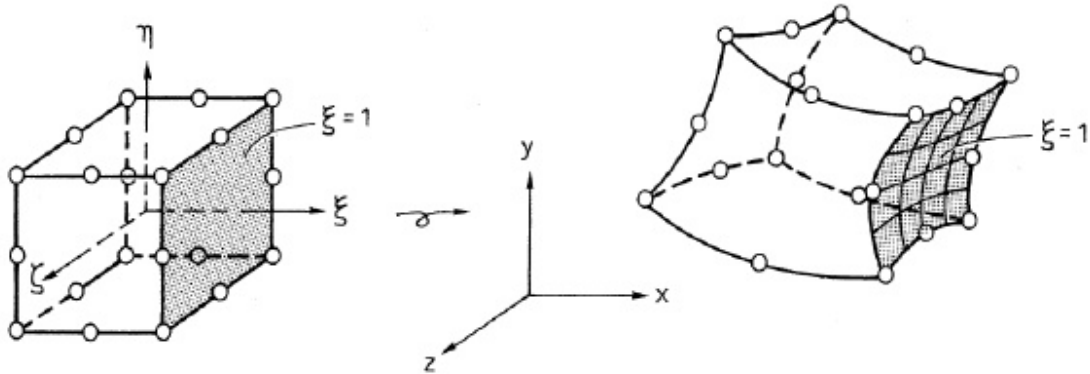


Figure 4.1: Twenty-node three dimensional isoparametric brick element [14].

4.2 Structural dynamics

An introduction to structural dynamics- and vibrations theory, as well as the theory behind buckling analysis is given in this section. For further reading about structural dynamics see [15].

4.2.1 Springs

The force needed to extend or compress a spring a distance, is linearly proportional to that distance. This relation is described by Hooke's law according to eq. (4.8)

$$f_s = ku \quad (4.8)$$

where k is the stiffness, f_s is the force with and u is the displacement [14].

4.2.2 Modelling rubber boundaries

When modelling rubber boundaries the rubber can be replaced by springs with equal stiffness. By doing this, the stiffness of the rubber will be approximated to a few springs. This prevents the FE-analysis from calculating the modeshapes of the rubber and instead calculating the modeshapes of the entire system. The stiffness of a spring element is calculated according to eq. (4.9)

$$k = \frac{EA}{L} \quad (4.9)$$

where E is the elasticity of the rubber, A is the area of the rubber and L is the thickness of the rubber [14].

4.2.3 Steady state

In a steady state solution the dynamic system is transformed into a time independent system of equations for the amplitudes. Consider the undamped system in eq. (4.10).

$$\mathbf{M}\ddot{\mathbf{u}} + \mathbf{K}\mathbf{u} = \mathbf{f}_0 \sin(\omega t) \quad (4.10)$$

This system can be solved using a trial solution according to eq. (4.11), [16].

$$\mathbf{u} = \mathbf{u}_0 \sin(\omega t) \quad (4.11)$$

The second derivative of the displacement gives the acceleration according to eq. (4.12)

$$\ddot{\mathbf{u}} = -\omega^2 \mathbf{u}_0 \sin(\omega t) \quad (4.12)$$

Inserting eq. (4.11) and eq. (4.12) in eq. (4.10) gives the steady state solution for an undamped system according to eq. (4.13), [16].

$$(-\mathbf{M}\omega^2 + \mathbf{K})\mathbf{u}_0 = \mathbf{f}_0 \quad (4.13)$$

4.2.4 Damping

The process which makes the free vibrations diminish is called damping. The damping dissipates the vibration energy from the system due to different mechanisms. It is impossible to establish all the mechanisms in a structure that contribute to the damping. Some examples of damping are energy dissipation from repeated elastic straining, internal friction when a solid is deformed, and opening and closing of micro cracks in concrete when the structure is subjected to a vibration load [15].

Since it is difficult to determine all the mechanisms that contribute to damping, the damping in structures is idealized. In a MDOF-system the damping can be described with the equation

$$\mathbf{f}_D = \mathbf{C}\dot{\mathbf{u}} \quad (4.14)$$

where \mathbf{C} is the damping coefficient with the unit of Ns/m, \mathbf{f}_D is the forces with the unit N and $\dot{\mathbf{u}}$ is the velocity with the unit m/s [15].

The equation of motion for a damped system can be seen in eq. (4.15), [16].

$$\mathbf{M}\ddot{\mathbf{u}} + \mathbf{C}\dot{\mathbf{u}} + \mathbf{K}\mathbf{u} = \mathbf{f}_0 \sin(\omega t) \quad (4.15)$$

In a damped system the displacements will also be harmonic but with a phase lag relative to the force. A damped system can be described with complex notation which takes the phase lag into account. Using complex representation the displacements can be rewritten according to eq. (4.16), [16].

$$\mathbf{u} = \mathbf{u}_0 e^{i\omega t} \quad (4.16)$$

The first- and second derivative of the displacement gives the velocity and acceleration according to eq. (4.17) and (4.18).

$$\dot{\mathbf{u}} = i\omega \mathbf{u}_0 e^{i\omega t} \quad (4.17)$$

$$\ddot{\mathbf{u}} = -\omega^2 \mathbf{u}_0 e^{i\omega t} \quad (4.18)$$

Inserting eq. (4.17) and eq. (4.18) in eq. (4.15) gives the steady state solution for a damped system according to eq. (4.19).

$$(-\mathbf{M}\omega^2 + i\omega\mathbf{C} + \mathbf{K})\mathbf{u}_0 = \mathbf{f}_0 \quad (4.19)$$

4.2.5 Rayleigh damping

The basis for Rayleigh damping is that for low eigenfrequencies the damping primarily depends on the mass and for high eigenfrequencies damping primarily depends on the stiffness [15], as can be seen in Figure 4.2.

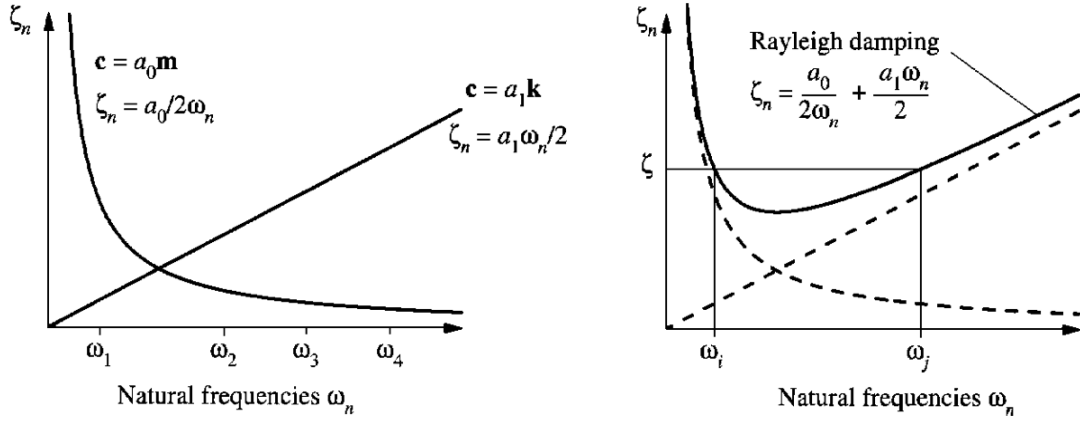


Figure 4.2: Rayleigh damping [15].

The damping ratio for the n^{th} mode of a system is calculated with eq. (4.20)

$$\zeta_n = \frac{a_0}{2} \frac{1}{\omega_n} + \frac{a_1}{2} \omega_n \quad (4.20)$$

where a_0 and a_1 are Rayleigh coefficients, ζ_n is the n^{th} damping ratio and ω_n is the n^{th} eigenfrequency [15].

The coefficients a_0 and a_1 can be determined from two angular frequencies ω_i and ω_j as shown in eq. (4.21).

$$\begin{bmatrix} \frac{1}{2\omega_i} & \frac{\omega_i}{2} \\ \frac{1}{2\omega_j} & \frac{\omega_j}{2} \end{bmatrix} \begin{bmatrix} a_0 \\ a_1 \end{bmatrix} = \begin{bmatrix} \zeta_i \\ \zeta_j \end{bmatrix} \quad (4.21)$$

For Rayleigh damping the \mathbf{C} matrix consists of the Rayleigh coefficients according to eq. (4.22), [16].

$$\mathbf{C} = a_0 \mathbf{M} + a_1 \mathbf{K} \quad (4.22)$$

4.3 Buckling analysis

In the eigenvalue buckling problem, the loads sought after are the ones for which the stiffness matrix of the structure becomes singular, so that the problem

$$\mathbf{K}\mathbf{u} = \mathbf{0} \quad (4.23)$$

has nontrivial solutions [19]. \mathbf{K} is the tangent stiffness matrix when the loads are applied and \mathbf{u} are the nontrivial displacement solutions. The magnitude of the loading required to achieve buckling is scaled by the load multipliers λ_i found in the eigenvalue problem

$$(\mathbf{K}_0 + \lambda\mathbf{K}_\Delta)\mathbf{u} = \mathbf{0} \quad (4.24)$$

where \mathbf{K}_0 is the stiffness matrix corresponding to the base state, \mathbf{K}_Δ is the differential initial stress and load stiffness matrix due to the incremental loading pattern, λ are the eigenvalues and \mathbf{u} are the buckling mode shapes [19].

4.4 Abaqus modelling

To model the structural components regarding its strength and dynamic response, the software Abaqus CAE is used in this work. Abaqus is a software suite for finite element analysis and computer aided engineering, based on the scripting language Python. Abaqus CAE is a user interface that can be used both for modelling of mechanical components and assemblies as well as visualizing the finite element analysis results.

All elements that were used for modelling of the glass structure in this report in Abaqus were deformable 20 node quadratic 3D solids. The material properties were chosen as the material properties given in Chapter 3. The interlayers were considered to be ideally plastic materials and were allowed to deform plastically.

5 Eurocode and standards

The design values considering the maximum strength of glass, the ultimate limit state (ULS) and the serviceability state (SLS) are calculated in this chapter. The technical rules used are all developed by the European Committee for Standardisation, so called Eurocode. Vibration analysis is also discussed in this chapter.

5.1 Design value of strength for heat strengthened glass

The design value of strength for a heat strengthened glass material is calculated according to the equation for pre stressed glass in Eurocode [20]

$$f_{g;d} = \frac{k_{mod}k_{sp}f_{g;k}}{\gamma_{M;A}} + \frac{k_v(f_{b;k} - f_{g;k})}{\gamma_{M;v}} \quad (5.1)$$

where k_{mod} is a factor concerning the load duration, k_{sp} is a factor for the glass surface profile and $f_{g;k}$ is the characteristic value of the bending strength. The material partial factor is called $\gamma_{M;A}$ for annealed glass. The factor k_v does consider strengthening of pre-stressed glass, $f_{b;k}$ is the characteristic value of pre-stressed glass and $\gamma_{M;v}$ is a material partial factor for surface pre stressed glass.

Values for the calculation of the design value for heat strengthened glass are seen in Table 5.1. All values are found in [20]. The variable k_{mod} is chosen considering the worst case scenario to be a personnel load with 30 seconds of duration. This value was chosen out of the condition that it is not likely that people in a worst case scenario will stay longer than a few seconds on the same part of the floor.

Parameter	Value	Source
k_{mod}	0.89	Table 6
k_{sp}	1.0	Table 5
$f_{g;k}$	45 MPa	Section 8.1.1
$\gamma_{M;A}$	1.8	Table 2
k_v	1.0	Table 8
$f_{b;k}$	70 MPa	Table 7
$\gamma_{M;v}$	1.2	Table 2

Table 5.1: Values for calculation of the design value for heat strengthened glass [20].

Insertion of these values into eq. (5.1) gives the design value of strength for heat strengthened glass.

$$f_{g;d} = \frac{0.89 \cdot 1.0 \cdot 45 \cdot 10^6}{1.8} + \frac{1.0(70 \cdot 10^6 - 45 \cdot 10^6)}{1.2} \rightarrow f_{g;d} = 43.1 \text{ MPa}$$

5.2 Design of the glass structure

5.2.1 Design value for loading in ultimate limit state

According to Eurocode the load to be applied on a structure in the ultimate limit state shall be calculated with eq. 6.10b in [13], as can be seen in eq. (5.2)

$$q_d = \gamma_d 1.2 G_{kj,sup} + \gamma_d 1.5 Q_{k,1} \quad (5.2)$$

where γ_d is a factor concerning the safety class, $G_{kj,sup}$ is the permanent loading and $Q_{k,1}$ is the variable concentrated loading. Depending on the worst case scenario the variable load can be placed either as a concentrated load or as a distributed load. If the variable load is introduced as a distributed load, the parameter $Q_{k,1}$ is replaced with $q_{k,1}$ in equation (5.2).

The factor γ_d is in this case 1.0, as the risk for personal injury is high. The factor $G_{kj,sup}$ varies depending on the weight of the structure. The characteristic value $Q_{k,1}$ is for a congregation area 3 kPa. These values are given in [13], Table 1.7.

5.2.2 Serviceability limit state

The load combination used for serviceability limit state is quasi-permanent loading. According to Eurocode, the load on a structure when exposed to long time loading is calculated with equation 6.16b [13], as can be seen in eq. (5.3).

$$q = 1.0 G_{k,j} + \psi_{2,j} q_{k,i} \quad (5.3)$$

where $G_{k,j}$ is the permanent loading, $\psi_{2,j}$ is a factor concerning variable loads, and $q_{k,i}$ is the variable loading.

The parameter $G_{k,j}$ varies depending on the weight of the structure. For a congregation area $\psi_{2,j}$ is 0.6, which is given in [13] at Table 1.6. The characteristic $q_{k,i}$ for a congregation area is 3 kPa. The values are to be found in [13], Table 1.7.

5.3 Vibration analysis

The vibration analysis will be performed as described in chapter 2 in *Acceptance criteria for human comfort*, by [18]. The acceleration at an arbitrary node in the structure is multiplied with a reduction factor α_i according to Table 5.2. Which one of the factors the acceleration is multiplied with is dependent on what frequency that is exciting the structure. In [18] the first frequency interval does not stop where the second frequency interval starts and the second frequency interval does not stop where the third frequency interval starts and so on. Therefore to cover the entire frequency span the frequency intervals are slightly modified to start where the previous interval stops as can be seen in Table 5.2.

Frequency interval (Hz)	1.6-3.2	3.2-4.8	4.8-6.4	6.4-8.8
α_i	0.5	0.2	0.1	0.05

Table 5.2: Vibration reduction factors [18].

Apart from multiplying the acceleration with α_i the stated calculations also have to take the persons moving around on the floor in consideration. This is taken into account by multiplying the weight of a person, typically 700 N with the square root of the number of persons moving around on the floor [18]. The square root takes the uncorrelated movement of the persons into consideration. For example if nine persons are walking uncorrelated it gives the same effect on the vibrations as three persons walking correlated.

When calculating the accelerations on the structural element the load is to be put as a total of 1 N. The accelerations of the structural element is linearly proportional to the load applied which leads to simple calculations; in this case the loads from persons moving on the floor will hence be multiplied by 1.

After multiplying the acceleration in an arbitrary node of the structure with α_i , the weight of a person and the square root of the number of persons moving on the structure, the value gained is divided with the acceleration of gravity to get the node-acceleration in relation to the acceleration of gravity. This can be seen in eq. (5.4).

All the calculated values of the node-accelerations related to the acceleration of gravity are then compared with approved values of vibrations for different activities. The complete equation used for calculating the vibrations is

$$\frac{a}{g} = \frac{g_{person} \alpha_i \alpha_i \sqrt{n_{persons}}}{g} \quad (5.4)$$

where g_{person} is the weight of an average person estimated to 700 N, α_i is the acceleration at a specific frequency, α_i is a reduction factor within a frequency interval, g is the acceleration of gravity assumed to be 9.81 m/s² and $n_{persons}$ is the number of persons moving on the floor.

6 Design of glass plates

In this chapter the design of the glass plates that are placed on the glass beams in the floor-structure is performed. The analysis was carried out when a uniformly distributed load or a concentrated load were acting on the surface. Requirements concerning deflection were also considered in the analysis. The behaviour of a plate when cracking occurs through the section was considered as well.

6.1 Estimation of a glass plate

The maximum moment capacity of a rectangular beam is given by [21], as eq. (6.1)

$$M = \sigma \cdot \frac{bh^2}{6} \quad (6.1)$$

and the maximum moment at the midpoint of a simply supported beam subjected to a uniformly distributed load is given by [13], as eq. (6.2).

$$M = \frac{qL^2}{8} \quad (6.2)$$

where M is the maximum moment, σ is the maximum normal stress, b is the width, h is the height, L is the length and q is the line load.

A rough estimation of a glass plate's dimensions was carried out with a calculation, where one meter of a glass plate in width where calculated as a beam. A roughly estimated load of 6 kPa was assumed to act along a plate. Combining eq. (6.1) and eq. (6.2) gives

$$\frac{6 \cdot 10^3 \cdot 1.5^2}{8} = 43.1 \cdot 10^6 \cdot \frac{1 \cdot h^2}{6} \rightarrow h = 0.015 \text{ m}$$

15 mm is a rather thin glass layer and the dimension may be higher when more accurate calculations are carried out. To make the profile efficient and resistant if cracking would occur, it was desirable to have the laminate a bit out from the centre of the section. A decision was made to have three or four layers of glass laminated together with 1.52 mm SGP.

The shear capacity of a cross section was investigated and is given by [13], as eq. (6.3)

$$\tau_y = \frac{VS_y}{Ib_y} \quad (6.3)$$

where S_y is the first moment of area, V is the shear force, I is the second moment of area and b_y is the width. To calculate the maximum shear capacity of a rectangular beam, eq. (6.3) can be written as eq. (6.4).

$$\tau = \frac{V \cdot \frac{h}{2} \cdot \frac{h}{4}}{\frac{bh^3}{12} \cdot b} = \frac{3V}{2hb} \quad (6.4)$$

The maximum shear force of a simply supported beam subjected to a uniformly distributed load is given by [13] as eq. (6.5)

$$V = \frac{qL}{2} \quad (6.5)$$

where q is the uniformly distributed load and L is the length of the beam. Combining eq. (6.4) and eq. (6.5) gives the required height of the plate when considering shear capacity.

$$\tau = \frac{3 \cdot \frac{qL}{2}}{2hb} \rightarrow h = \frac{3qL}{4\tau b} = \frac{3 \cdot 6 \cdot 10^3 \cdot 1.5}{4 \cdot 43.1 \cdot 10^6 \cdot 1} = 0.00016 \text{ m}$$

6.1.1 Conclusion considering shear force

The height required of the section to take the shear stresses was just a fraction of the height required to take the moment. An assumption was made that the moment capacity of the cross section would be the design basis of the plates.

6.2 Analysis of stresses and deflections

6.2.1 Abaqus modelling

The elements which were chosen for modelling the glass plates were 20 node quadratic brick elements with reduced integration. The material properties were decided to be as stated in Chapter 3. The SGPs were assumed to deform as an ideally plastic material after reaching the stress 23 MPa where plastic deformation begun.

The glass plates were analysed using a static load step. In this analysis the plates were modelled as simply supported, see Figure 6.1. At the bottom of both ends, the edge was prevented from moving in the z-direction. The plates were prevented to move in the x-direction at the bottom of one end and prevented from moving in the y-direction in one node at the bottom of each end. These boundary conditions allowed the plates to expand in the longitudinal and lateral directions but prevented rigid body displacements.

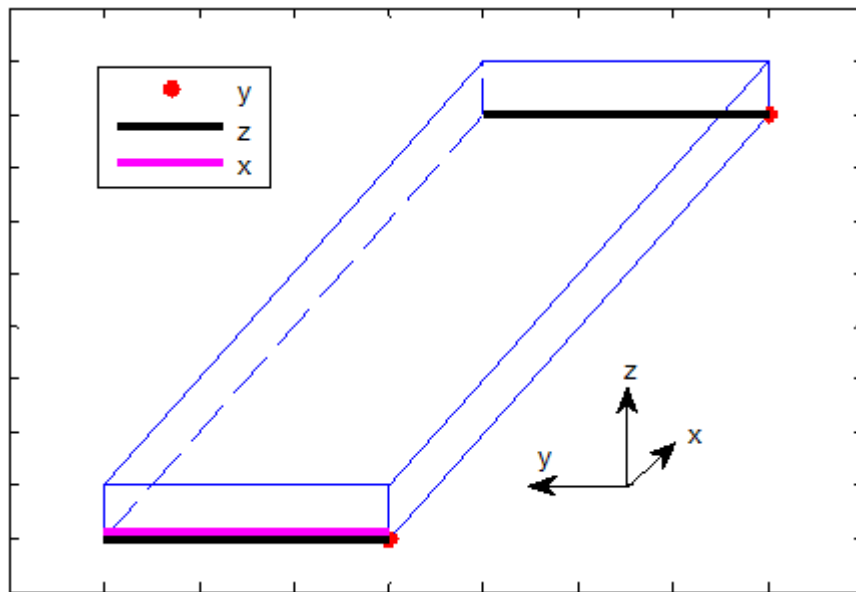


Figure 6.1: Boundary conditions for the glass plates.

6.2.2 Meshing of the glass plates

Calculations to verify the needed mesh size for a given glass plate were carried out to decide the meshing size needed for a good approximation of the stresses. The analyses were performed on a plate exposed to a distributed load of 0.9 kPa or a concentrated force of 4.5 kN on an area of 50x50 mm² in the middle of the plate at one edge. The meshed plate is visualized in Figure 6.2.

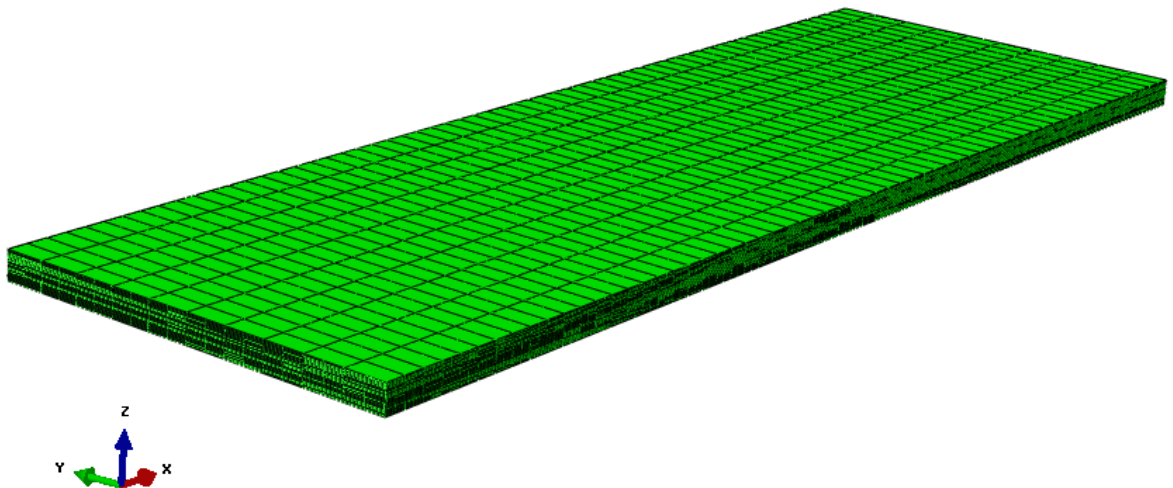


Figure 6.2: Meshing of a plate.

First the number of elements required for the xy-plane was determined by varying the size in the xy-plane and keeping the mesh in the z-direction to be one element in all layers through the entire plate. In Table 6.1 an evaluation where the global mesh size in the xy-plane is varied, is compared with a mesh where the y-direction is decided to be 50 mm and the x-direction varies.

Mesh width (mm)	50	25	12.5
Stress (MPa), global mesh	28	28.9	29.2
Stress (MPa), mesh constant 50 in y-direction, varies in x-direction	28	28.9	29.1

Table 6.1: Comparison horizontal meshing.

In Table 6.2 the results from an evaluation is shown where a 50x12.5 mesh and a 50x25 mesh like the ones described above is compared for various mesh sizes in the z-direction. Three different cases were tested where each glass plate was divided into 1, 2 and 3 elements in the thickness direction for each material layer.

Number of elements/layer	1	2	3
Stress (MPa), mesh: 50x12.5, vertical varies	29.1	34.2	36
Stress (MPa), mesh: 50x25, vertical varies	28.9	34	35.7

Table 6.2: Comparison of 50x12.5 and 50x25 in vertical meshing.

A conclusion was reached that a meshing pattern of 50x25 is enough in the xy-plane. The required meshing in the z-direction was also decided, in Figure 6.3 the results from an evaluation is shown. The horizontal axis shows the number of elements that each glass layer was divided into. When divided into 8 numbers of elements per layer, the SGP-layers were divided as well, into 2 layers per element.

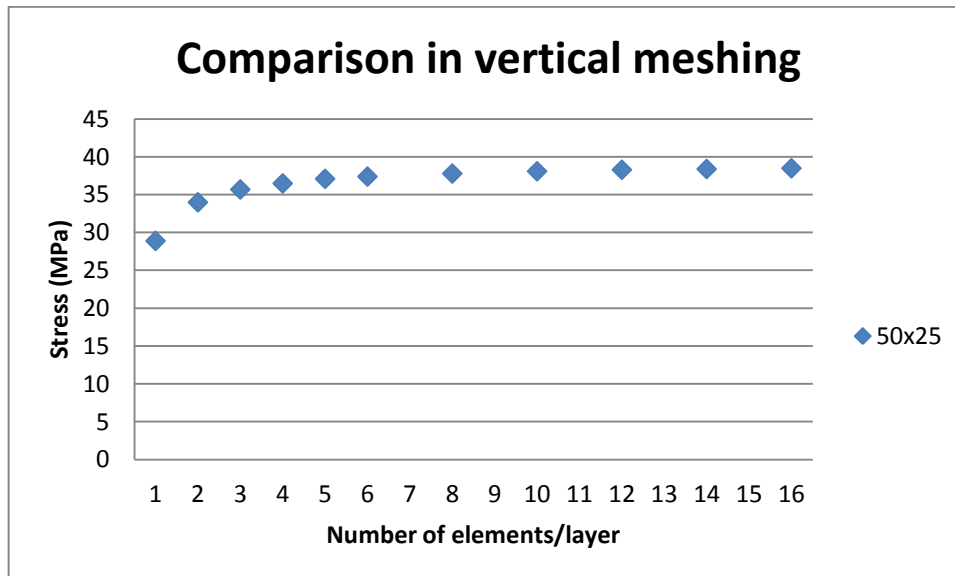


Figure 6.3: Comparison in vertical meshing.

The meshing in the vertical direction was decided so that each glass part had 3 elements. This mesh size was considered as a meshing accurate enough to be used when calculating the stresses in the plates. The meshing does not provide an exact result, but a good estimation to fit the purpose.

6.2.3 Description of the analysis

The stresses and the deflections in the glass plates were to be decided. Different plate dimensions were modelled and tested. One single plate had the dimension of 1.5x0.5

m in size. Firstly a laminated plate with three equally thick glass layers with interlayers of SGP were modelled and secondly a laminated plate with four glass layers consisting of two differing thicknesses. The laminated plates were modelled as simply supported.

Glass laminates with five types of sections were analysed, see Figure 6.4 . The first consisting of three 8 mm glass layers, the second of three 10 mm glass layers and the third of three 12 mm glass layers. The fourth section tested consisted of two 10 mm glass layers closest to the centre of the laminate and two 8 mm glass layers outermost. The fifth section tested consisted of two 12 mm glass layers closest to the centre of the laminate and two 8 mm layers outermost.

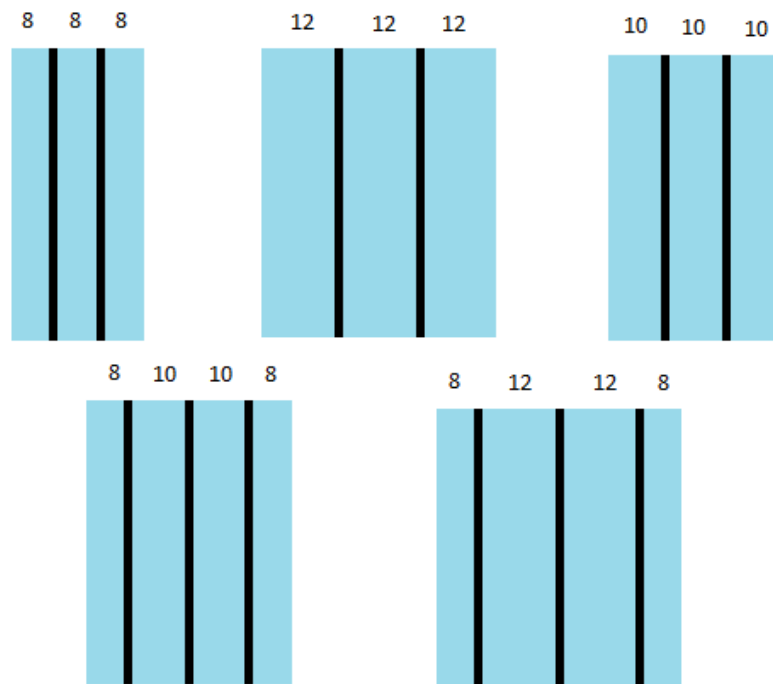


Figure 6.4: Glass plates to be analysed.

Stresses and deflections in the different sections were analysed by means of the FE-method for two types of loading. The first was a distributed load of 4.5 kPa, the second a concentrated load of 4.5 kN. The concentrated load was placed on a surface of a 50x50 mm square area at the centre of the plate at an edge, which was the worst location for a concentrated load on the plate. Concerning loads in the serviceability state a distributed load of 1.8 kPa was employed. Self weight was added to all load cases.

Table 6.3 shows all data with forces acting on the plates. The loads that were imposed to the plates are given and calculated according to sections 5.2.1, 5.2.2 and [13].

Dimension Plate type (mm)	ULS			SLS		
	Imp. load kPa	Imp. load kN	Self weight kPa	Imp. load kPa	Imp. load kN	Self weight kPa
3x8	4.5	4.5	0.7	1.8	1.8	0.6
3x10	4.5	4.5	0.9	1.8	1.8	0.8
3x12	4.5	4.5	1.1	1.8	1.8	0.9
2x8+2x10	4.5	4.5	1.1	1.8	1.8	0.9
2x8+2x12	4.5	4.5	1.2	1.8	1.8	1.0

Table 6.3: Loads acting on the plates.

Analyses concerning loading of the five plates in ULS were performed for both a distributed load and a concentrated load. The maximum principal stress in the glass was determined in order to verify that it did not exceed the allowed stress of 43.1 MPa.

Analyses concerning loading of the five plates in the SLS was also made for a distributed load and a concentrated load. Maximum deflection was determined to verify that did not exceed a deflection of $L/300$, which is a commonly used, rather high requirement [13].

An analysis was also carried out to verify the durability of the section when cracking has occurred. This analysis was only performed on one of the plates.

6.3 Results from the static analyses

The results from the static analyses for the five different plates in ULS, when exposed to a distributed load or a concentrated load, are shown in Figure 6.5.

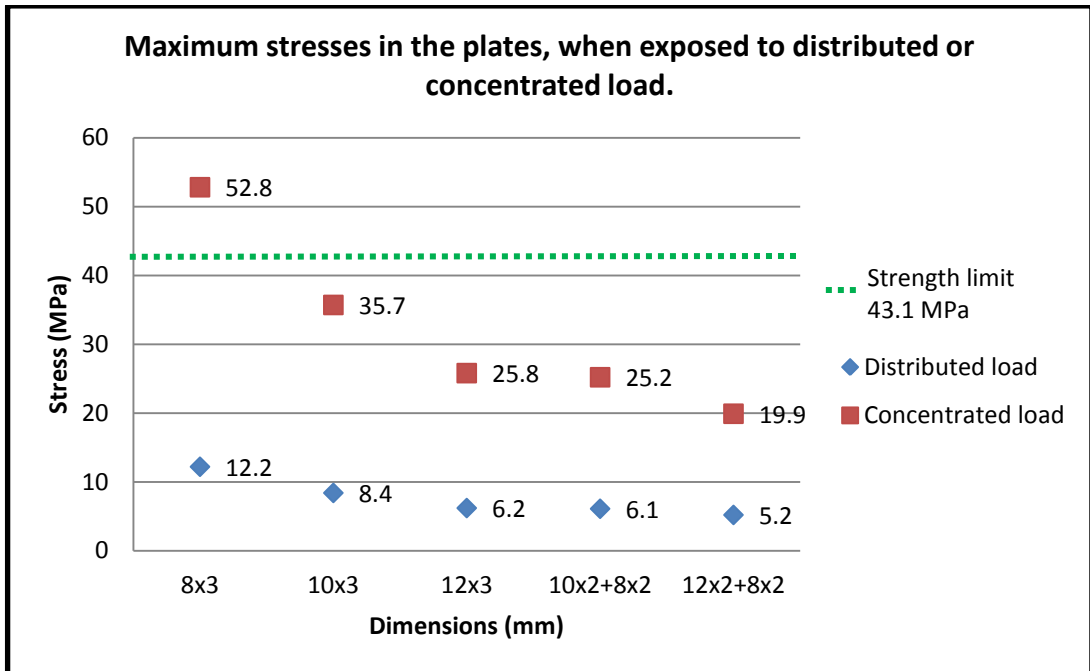


Figure 6.5: Maximum stresses in the plates, when exposed to distributed- and concentrated load.

The results of the analyses considering the five different plates concerning the maximum deflection when exposed to a distributed load or a concentrated load in SLS are shown in Figure 6.6.

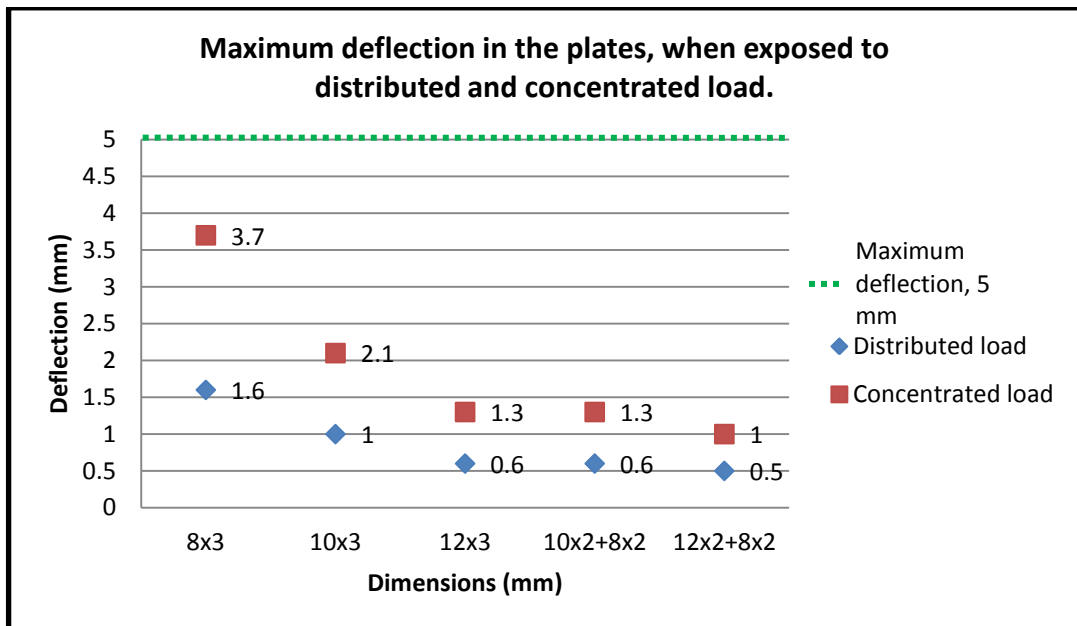


Figure 6.6: Maximum deflection in the plates, when exposed to distributed- and concentrated load.

6.3.1 Conclusion static analysis

The concentrated loads gave higher stresses and larger deflections in the glass than the distributed loads. All of the analysed glass plates, except the 3x8 mm plate, could carry the loads without reaching critical stresses in the glass of 43.1 MPa and without exceeding the maximum deflection of 5 mm.

6.4 Cracked glass plates

It is important for safety reasons that the glass floor does not collapse in case cracking occurs. To verify that the glass floor could carry the loads with cracks present, a comparison with a laboratory testing and an approximate calculation was performed.

Calculations concerning cracked glass plates are rather complicated. If cracking occurs in a single glass layer it is difficult to predict how a crack will develop through the material and if the crack will break through all layers or stay in one layer. If the cracking starts in one single layer and breaks through it, fracture mechanics is necessary to validate if the crack will continue through the next layer or stop at the interlayer between the glass layers. The exact pattern of the cracking is needed for the calculations to be correct and the pattern concerning glass is hard to decide. The residual strength of the glass plate may, however, be estimated for a worst case scenario.

Several test studies have been carried out concerning broken laminated glass plates. In [3] a canopy of heat strengthened glass is subjected to a uniformly distributed static load of 1.5 kPa, see Figure 6.7. The dimension of the canopy was 1x1 m² and it consisted of two 8 mm thick layers of heat strengthened glass laminated together with 1.52 mm SGP. The plates were completely cracked before the load was applied on the section and were acting for 24 hours resulting in that the plate was still able to carry the load.



Figure 6.7: Loading of cracked glass plate. Testing carried out by [3].

6.5 Analytically calculated strength of cracked glass plates

The study carried out by [3] shows that two cracked glass layers, laminated together with 1.52 mm SGP, can carry a weight of 1.5 kPa for 24 hours. Therefore it should be realistic to consider four layers of glass, laminated together with 3 layers of SGP enough to carry at least three times the load. The profile consisting of 8-12-12-8 mm laminate will probably be enough to carry a distributed load of 4.5 kPa on a span of 1.5 m, when all the plates are completely cracked.

A calculation of a cracked glass plate was carried out on an 8-12-12-8 mm laminated plate, where the section was considered to be cracked. In order to calculate the strength of the cracked glass plates, an analytical calculation on a simplified model was carried out. To determine that the residual strength of the glass plate had sufficient moment capacity, the cracked section was compared with the moment generated from the loading. The cracked section can be seen in Figure 6.8.

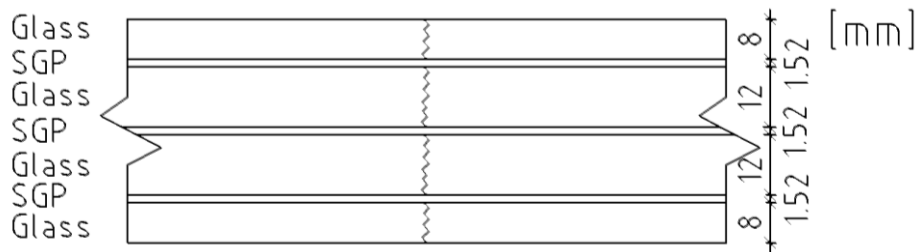


Figure 6.8: Cracked section of a glass plate.

In Figure 6.9 the stresses in the cross section can be seen before cracks have occurred. The glass will in this state take compressive- and tensile stresses. The interlayers will have a negligible impact on the stress distribution and are therefore not illustrated in this figure.

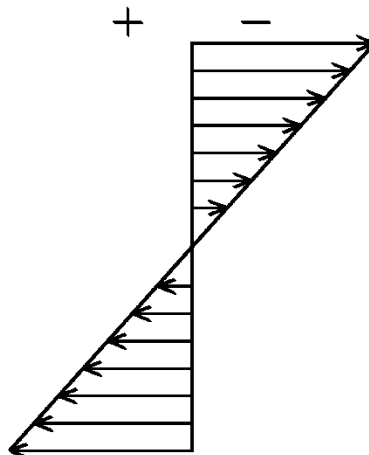


Figure 6.9: Stress distribution in uncracked section.

If the glass cracks it can still carry compressive stresses. The worst scenario would be that all the glass layers crack, leading to a redistribution of the stresses in the glass layers and in the interlayers. An assumption regarding this scenario is that the upper part of the top plate takes all the compressive stresses while the three interlayers take

the tensile stresses, as shown in Figure 6.10. The failure strength of the interlayer material is around 34.5 MPa according to [22]. The interlayers were assumed to be of an ideally plastic material. All of the interlayers in the model were assumed to have reached the failure strength of the material.

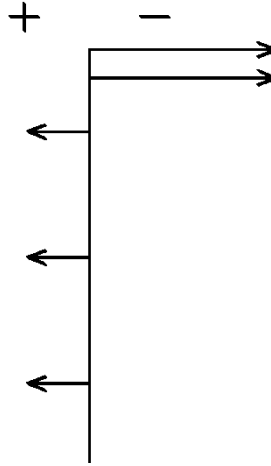


Figure 6.10: Stress distribution in cracked section.

A section of the cracked glass plate can be seen in Figure 6.11. All of the glass layers were cracked but the interlayers were assumed to remain intact. When the glass layers are cracked, the plate still has to carry the moment and shear forces from the loading. Considering the high compressive stresses that occurred in the top of the glass plate, an assumption was made that this would be enough to carry the shear force in the section, and no verification of the shear force capacity was performed.

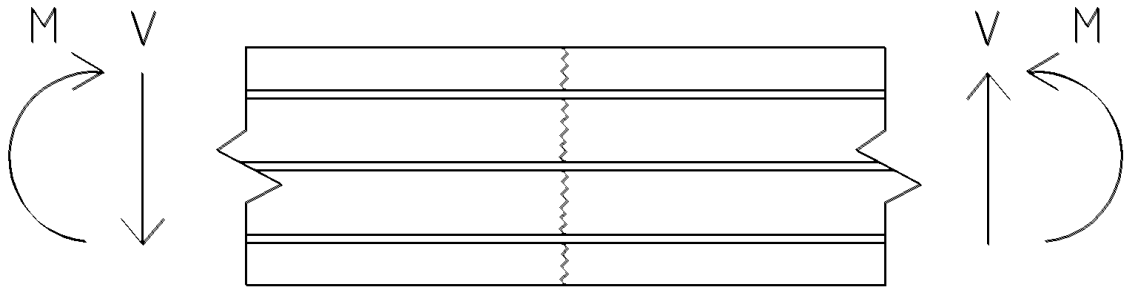


Figure 6.11: Cracked section of a glass plate.

The forces in the interlayers in Figure 6.12 were calculated per meter in the lateral direction of the plates. The stress in the top glass plate equals the stresses in the interlayers in order to achieve lateral equilibrium. The compressive stresses were assumed to be redirected around a joint in the upper part of the top glass layer. Moment equilibrium was implemented from the joint according to eq. (6.6)

$$M = \sigma t L_1 + \sigma t L_2 + \sigma t L_3 \quad (6.6)$$

where the failure strength limit of the interlayers was $\sigma = 34.5$ MPa, the thickness of the interlayers was $t = 1.52$ mm and L_i are levers to the interlayers, where $L_1 = 4.76$ mm, $L_2 = 18.28$ mm and $L_3 = 31.8$ mm.

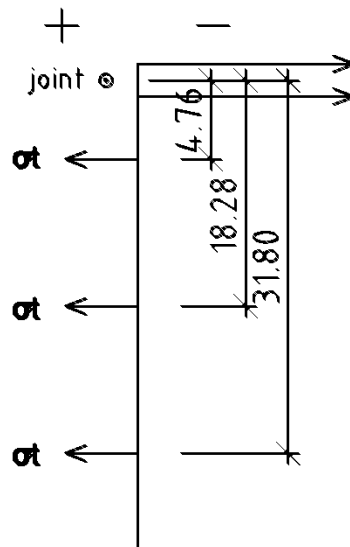


Figure 6.12: Stress distribution in the cracked section.

The values were inserted into eq. (6.6) and the moment capacity of the glass plates per meter was calculated according to eq. (6.7).

$$M = 34.5 \cdot 1.52 \cdot 8.76 + 34.5 \cdot 1.52 \cdot 21.52 + 34.5 \cdot 1.52 \cdot 34.28 \quad (6.7)$$

$$= 3386 \text{ Nm/m}$$

This moment capacity was compared with the moment generated from the loading. Assuming a concentrated force in the middle of the section the moment became

$$M = \frac{FL}{4} \quad (6.8)$$

where F was the line load acting on the glass plate, and L was the length of the plate.

The maximum loading per meter, was calculated as shown in eq. (6.9).

$$3386 = \frac{F \cdot 1.5}{4} \rightarrow F = 9029 \text{ N/m} \quad (6.9)$$

This corresponded to a concentrated force of 4.5 kN acting on half a meter of glass plate, which was about the same load as the imposed load in Table 6.3.

6.6 Conclusions and choice of glass plates

All plates modelled in Abaqus, except the one with 3x8 mm glass, had the required load bearing capacity uncracked. Considering cracked glass layers, tensile stresses cannot be taken, and thus knowing which layers that are cracked was important in order to perform an accurate analysis. However knowing how cracks are spreading through the laminated glass section is difficult and assumptions had to be made in order to make calculations. The assumption made was that all the glass layers were cracked which was considered the worst case scenario. The very approximate analytical calculation that was conducted in Section 6.5 showed that the glass floor will maintain its required load bearing capacity even when all the glass plates were cracked. The results in [3] and the results found in the analytical solution made a strong argument that the glass floor built up by 8-12-12-8 mm glass plates and 3x1.52 mm SGP interlayers would be able to carry the required loads even when cracking occurred in the glass plates.

If cracking occurs, the tensile forces acting on that plate have to be redistributed to the other glass plates and to the interlayers. The interlayers would deform plastically proportionally to time, as a consequence of the heavy local loads acting on the section. Testing on laminated plates however, as can be seen in [3], showed that no brittle breakage will develop in the section. People standing on one of the 1.5x0.5 plates will have plenty of time to move away from the cracked plate so that the glass can be replaced.

7 Design of glass beams

In this chapter the design of the beams in the system is performed. A static analysis of a beam was carried out to determine its load-bearing capacity. An evaluation concerning buckling of the beam was also performed.

7.1 Estimation of a glass beam

The maximum moment capacity of a rectangular beam is given by [21], as eq. (6.1)

$$M = \sigma \cdot \frac{bh^2}{6} \quad (7.1)$$

and the maximum moment at the midpoint of a simply supported beam subjected to a distributed load is given by [13], as eq. (6.2).

$$M = \frac{qL^2}{8} \quad (7.2)$$

where M is the maximum moment, σ is the maximum normal stress, b is the width, h is the height, L is the length and q is the line load.

A rough estimation of the glass beam's dimensions was carried out with a calculation where the load acting was assumed to be 6 kPa acting on a single beam. This gives a line load of $6 \cdot 1.5 = 9$ kN/m. Combining eq. (7.1) and eq. (7.2) gives

$$\frac{6 \cdot 10^3 \cdot 4^2}{8} = 43.1 \cdot 10^6 \cdot \frac{45 \cdot 10^{-3} \cdot h^2}{6} \rightarrow h = 0.19 \text{ m}$$

To be on the safe side a section height of the beam was chosen to be 250 mm. The shape of the reinforcement was decided to be quadratic with a dimension of $15 \times 15 \text{ mm}^2$ in stainless steel.

7.1.1 Conclusion considering shear force

As stated in Section 6.1 the shear force would not be a design basis of the plates. The same assumption was made considering the beams, that the moment capacity of the cross section would be a design basis of the beams.

7.2 Analysis of stresses, strains and deflections

7.2.1 Abaqus modelling

The elements that were chosen for modelling the glass plates were 20 node quadratic brick elements with reduced integration. The material properties were decided to be as stated in Chapter 3. The SGPs were assumed to deform as an ideally plastic material after reaching the stress 23 MPa where plastic deformation begun.

The glass beams were analysed using a static load step. The load was applied as distributed on top of a beam. In this analysis the beams were modelled as simply supported, see Figure 7.1. At the bottom of both ends the edge of a beam was prevented from moving in the y-direction. At the bottom of one end, the edge was prevented from moving in the z-direction. The steel is thus not prevented from moving in the z-direction, to get a more symmetrical deformation and to avoid stress concentrations. When modelled, a beam was prevented from moving in the x-direction at one node at the bottom of each end and along the entire longitudinal edge at the top. This allowed expansion in the x-direction. The boundary conditions can be seen in Figure 7.1.

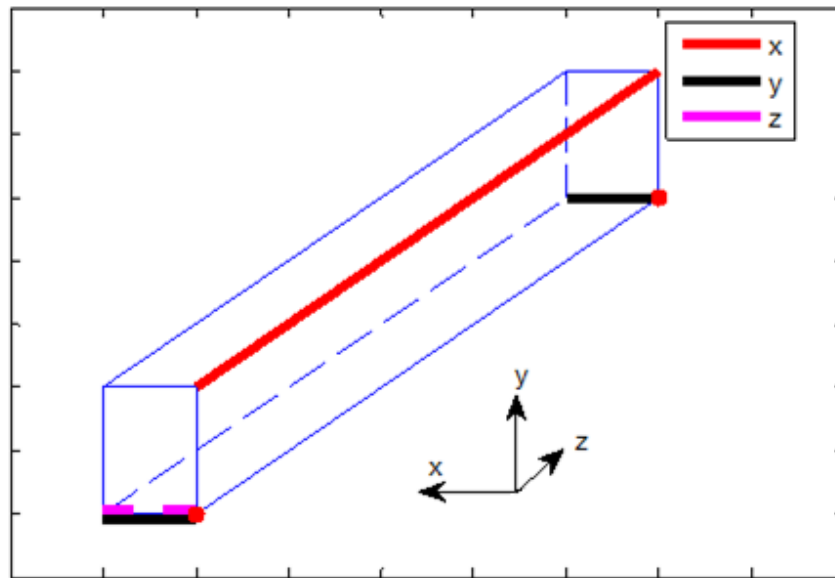


Figure 7.1: Boundary conditions for the glass beam.

7.2.2 Description of the analysis

The beam was 4 meters long and consisted of three 15 mm thick glass layers, laminated together with two 1.52 mm thick layers of SGP in between. The height of a beam was 250 mm. A quadratic 15x15 mm² reinforcement made out of steel acted in the bottom of the mid-section. The beam can be seen in Figure 7.2.

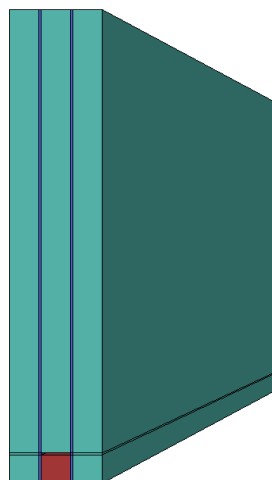


Figure 7.2: Glass beam.

One type of loading was performed in ULS. It was the already calculated distributed load of a glass plate acting on a beam, combined with the self weight of the beam. The beam was also tested concerning deflection in SLS. The load acting on the glass plates was multiplied with the length of a plate (1.5 m) to get total load acting on a beam.

The loads acting on a single beam are presented in Table 7.1 and calculated according to [13].

Dimension (mm)	ULS (kPa)		SLS (kPa)	
	Variable load	Self weight	Variable load	Self weight
3x15	140.5	40.0	56.2	33.3

Table 7.1: Loads acting on a single beam.

An analysis concerning loading in ULS was performed when a distributed load was applied. The maximum stress in the beam was decided to verify that it would not exceed the design strength value of heat strengthened glass, which was 43.1 MPa. The maximum stress in the steel as well as the maximum strain in the laminate was also to be decided.

An analysis concerning loading in SLS took part when a distributed load was applied. The maximum deflection in the beam was determined, and verification was carried out to confirm that it did not exceed a deflection of $L/300$ [13].

An analysis was carried out concerning a scenario in ULS when cracks had occurred throughout the midspan of a beam, causing a worst case scenario. The cracks did go through the cross-section from the bottom of the beam where tension did act until the top of the beam where compression started to act. The cracks developed in a triangular pattern through the section as can be seen in Figure 7.3. The modelling of the cracks is closely described in Section 7.2.3 and Section 7.2.4.

When the beam contained cracks, the maximum stress of the glass was decided in the section. The maximum strain in the interlayers was also calculated to verify that an extensive displacement did not occur. The maximum stress in the steel was finally decided.

7.2.3 Modelling of the cracks in the beam

When glass exceeds its tensile strength cracks occur. When cracks occur the glass can no longer carry tensile stresses, but the interlayers makes it possible for the glass to still take compressive stresses. The steel reinforcement has the purpose to carry the tensile stresses when cracks occur.

The cracks where shaped as thin lines that went through the vertical direction of the beam as can be seen in Figure 7.3. Looking at the shape of these cracks in Figure 7.3, the cracks were approximated by upside down triangles when they were modelled. An assumption was made that the glass within these triangles did not have any contributions to the load bearing capacity of the beam. This assumption was made as

the glass in the triangles was located in the tension member of the beam and hence could not carry any tensile stresses while surrounded by cracks.

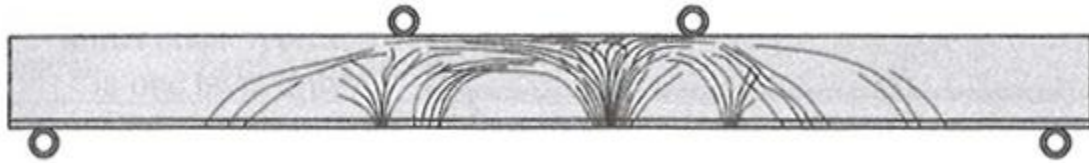


Figure 7.3: Cracks in a heat strengthened beam, [5].

When modelling the cracks in Abaqus an assumption was made that cracks only occur in the tension part of the beam, therefore the cracks were stopped when they reached the compression part of the beam. The exact height position in the beam where the cracking stopped was located through trial and error. By completing the analysis of the beam and hence visualizing the stresses in the longitudinal direction at the top of the cracks, one can see if there are tensile or compressive stresses. If there were tensile stresses, the cracks were raised, and if there were compressive stresses, the cracks were lowered. The modelling was considered completed when the top of the cracks was located at the neutral layer of the cross section, where the compressive and tensile stresses met.

The process of finding the neutral layer, where the cracks will stop developing, was carried out with trial and error and can be seen in Figure 7.4 - Figure 7.7. In these figures the steel reinforcement and the interlayers are hidden and only the glass is visible. The compressive stresses are shown as black and the tensile stresses are coloured.

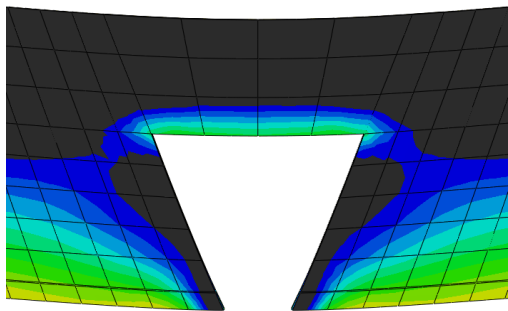


Figure 7.4: Cracks 10 cm from the top.

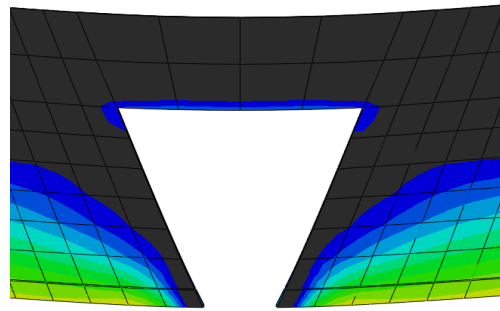


Figure 7.5: Cracks 8 cm from the top.

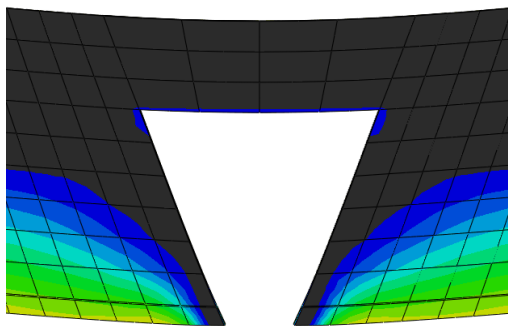


Figure 7.6: Cracks 7.5 cm from the top.

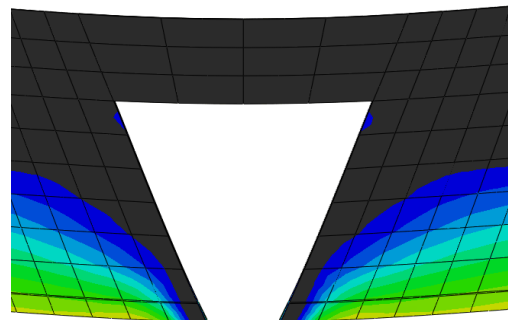


Figure 7.7: Cracks 7.0 cm from the top.

In Figure 7.4 the height of the cracks was decided to be 10 cm from the top. This crack height was too low as the top of the cracks contained tensile stresses, thus the cracks needed to be raised.

In Figure 7.5 the cracks were raised to be 8 cm from the top of the beam. As tensile stresses still existed in the top of the cracked section, the cracks needed to be raised further.

In Figure 7.6 the cracks were raised to be 7.5 cm from the top of the beam. As tensile stresses still existed in the top of the cracked section, but was about to shift to compressive stresses, the top of the cracks were almost placed at the neutral layer. However since the top of the cracks still contained tensile stresses it was possible for the cracks to go further up through the section. Therefore the cracks were raised a bit further.

The cracks were raised another 0.5 cm which can be seen in Figure 7.7. As can be seen, the top of the cracks only contained compressive stresses, which meant that the cracks would not go further up, and thus the correct height of the cracks was found.

This was an example of how the cracks were modelled in Abaqus. The cracks had a different height, depending on the load acting, the span of the beam, and the dimension of the beam. Figure 7.4 - Figure 7.7 was made in ULS on the 4 m long beam containing three 15 mm glass plates with two SGP interlayers in between. The crack height was different concerning modelling of the beams from the test study [5] as can be seen in Section 7.5, since they differed in applied load, dimension and span.

As can be seen in Figure 7.4 - Figure 7.7 the top of the beam takes compressive stresses. An assumption was made that the compressive part of the beam takes the shear stresses when the cross section is cracked. No further analysis concerning the shear stresses in the beam was carried out.

7.2.4 Modelling of multiple cracks in the beam

More than one set of cracks can occur, therefore an investigation was carried out concerning three sets of cracks. Figure 7.8 shows one beam with one set of cracks and one beam with three sets of cracks.

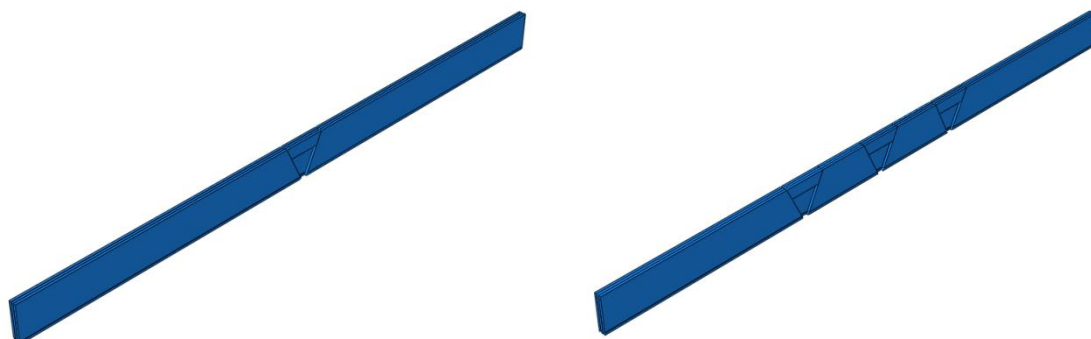


Figure 7.8: Beams with one and three sets of cracks.

To decide whether multiple cracks present a more unfavourable scenario some comparisons were carried out between the beams. The stress in the glass, the stress in

the steel, the strain in the SGP and the total deflection of the beams was compared. All these comparisons considered the maximum values and the results can be seen in Table 7.2.

	Stress glass (MPa)	Stress steel (MPa)	Strain interlayer (%)	Deflection (mm)
1 crack	39	364	14	8
3 cracks	39	363	14	10

7.2: Comparison between one- and three sets of cracks.

As shown in Table 7.2 it did not make much of a difference if there were one or multiple cracks in a beam. The deflection did vary a bit, but when a beam is cracked, people will be evacuated from the glass floor and the deflection that has appeared will not to a great extent impact the ability to perform the evacuation.

Since multiple cracks in the beam did not matter that much, the further analyses of the beam were only carried with one set of cracks.

7.3 Analysis of buckling

7.3.1 Abaqus modelling

The buckling analysis of a beam was carried out with use of two steps in Abaqus. The first step was a static load step, which introduced a deformation in the beam. The second step was a buckling step which performed a buckling analysis of the beam.

In the static load step a distributed load according to Table 7.1 was applied on top of the beam. Another load of 1000 N was applied in the lateral direction in the midspan of the beam. This force introduced a deformation to the beam before the buckling analysis was carried out. The option to perform the analysis using large deformations was also chosen in Abaqus.

In the buckling step a distributed load of 1 Pa was applied on top of the beam. In the buckling analysis, a requested number of eigenfrequencies and eigenmodes were calculated. In order to get the load at which the mode shapes occurred, the applied load was multiplied with the eigenvalue of the mode shape. Having the load as 1 Pa was convenient since the load at which the mode shapes occurred at could be determined directly from the eigenvalue, since it was multiplied with the load 1 Pa.

To better simulate the real boundaries of the beam, boundary conditions were changed to consist of rubber which had the form of a U with a plate on the back. Springs were introduced to simulate the rubber at these boundaries as problems with eigenvalues and eigenfrequencies occurred in the rubber layer when rubber as material was modelled as 3d solids. The material parameters of rubber were recalculated to be valid for the springs. These springs were the only boundary conditions on the beam which meant that the beam was not stabilized in the lateral direction on the top. In reality the beam will to some extent be stabilized in this direction due to the glass floor. However by ignoring the stabilizing addition from the glass floor, the analysis is performed using a more unfavourable case scenario.

7.3.2 Description of the buckling analysis

The stiffness of rubber is dependent on the dimensions of the rubber profiles. Since the rubber placed at the ends of the beam consisted of different sized rubber plates, they had different Young's moduli. A rubber boundary can be seen in Figure 7.9.

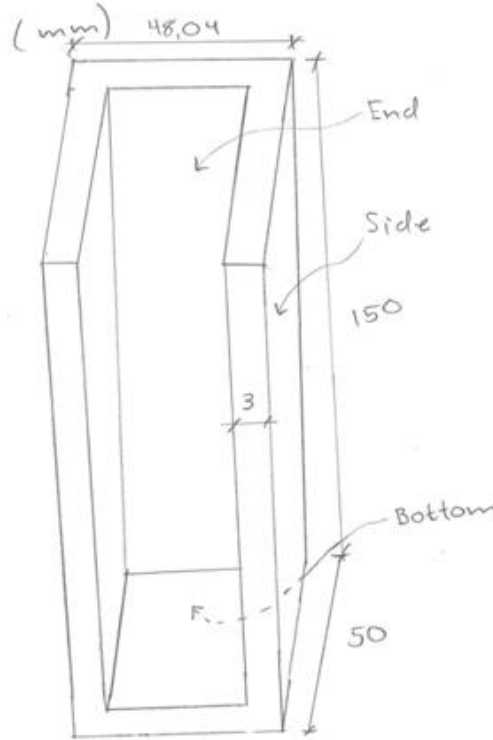


Figure 7.9: Rubber boundary.

The boundaries were assumed to consist of four rubber plates, one bottom plate, two side plates and an end plate. The stiffness was calculated according to [24]. A shape factor was calculated according to eq. (7.3) and the location of different areas can be seen in Figure 7.9.

$$\text{shape factor} = \frac{\text{loaded area}}{\text{force free area}} \rightarrow S = \frac{LB}{2t(L+B)} \quad (7.3)$$

The shape factor S was calculated for the rubber at the location of the end, side and bottom rubber boundary.

$$S_{End} = \frac{48.04 \cdot 150}{2 \cdot 3(48.04 + 150)} = 6.1$$

$$S_{Side} = \frac{50 \cdot 150}{2 \cdot 3(50 + 150)} = 6.3$$

$$S_{Bottom} = \frac{48.04 \cdot 50}{2 \cdot 3(48.04 + 50)} = 4.1$$

With the shape factors and the hardness of the rubber used, Young's moduli could be calculated. The EPDM rubber used in this report was assumed to have a hardness of 70 IRHD. Looking at the diagram in Figure 7.10 the following Young's moduli were found.

$$E_{End} = 250 \text{ MPa}$$

$$E_{Side} = 275 \text{ MPa}$$

$$E_{Bottom} = 125 \text{ MPa}$$

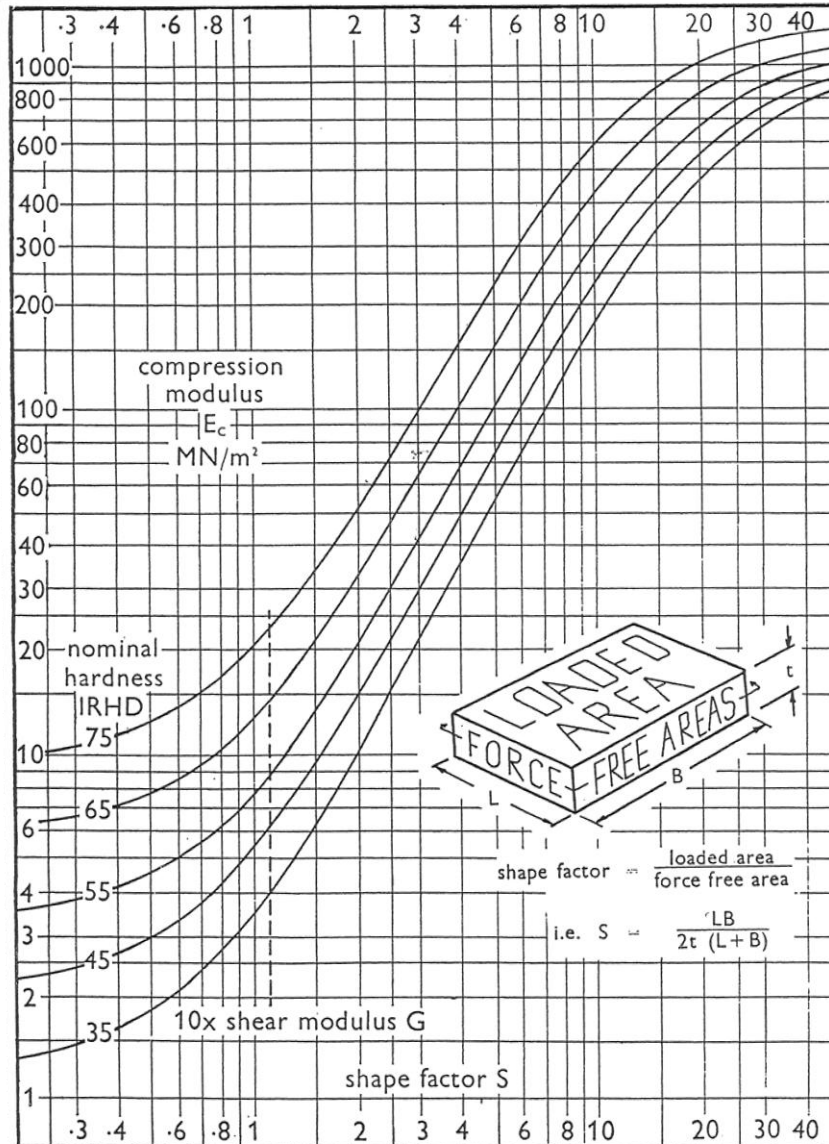


Figure 7.10: Definition of areas on loaded rubber [24].

The thickness of the rubber was decided to be 3 mm. The calculation concerning the stiffness was calculated as shown below.

$$k_{End\ rubber} = \frac{250 \cdot 10^6 \cdot 0.04804 \cdot 0.15}{0.003} = 600.5 \text{ MN/m}$$

$$k_{Side\ rubber} = \frac{275 \cdot 10^6 \cdot 0.05 \cdot 0.15}{0.003} = 687.5 \text{ MN/m}$$

$$k_{Bottom\ rubber} = \frac{125 \cdot 10^6 \cdot 0.05 \cdot 0.04804}{0.003} = 100.1 \text{ MN/m}$$

The springs were placed according to Figure 7.11, with 6 springs on each side of the beam, 6 springs on the end and 6 springs on the bottom. The stiffnesses were divided so that the outer springs each contained 1/8 of the stiffness and the springs in the middle each contained 2/8 of the stiffness in the respective directions. This refers to the springs located on the sides directed in the x-direction, springs on the bottom in the y-direction and springs on the ends in the z-direction.

Some nodes had spring stiffnesses in more than one direction, for example both nodes in the bottom corners of the beam had spring stiffnesses in all three directions. A rough explanation of the placement of the springs can be seen in Figure 7.11. The purpose of this figure is to explain where on the profile $k_{End\ rubber}$, $k_{Side\ rubber}$ and $k_{Bottom\ rubber}$ are defined, therefore all positions were not written in the figure. The stiffness values acting on the beam can be seen in Table 7.3.

Position	End, mid	End, outer	Side, mid	Side, outer	Bottom, mid	Bottom, outer
Stiffness (MN/m)	150.1	75.1	171.9	85.9	25.0	12.5

Table 7.3: Spring stiffness values on the beam.

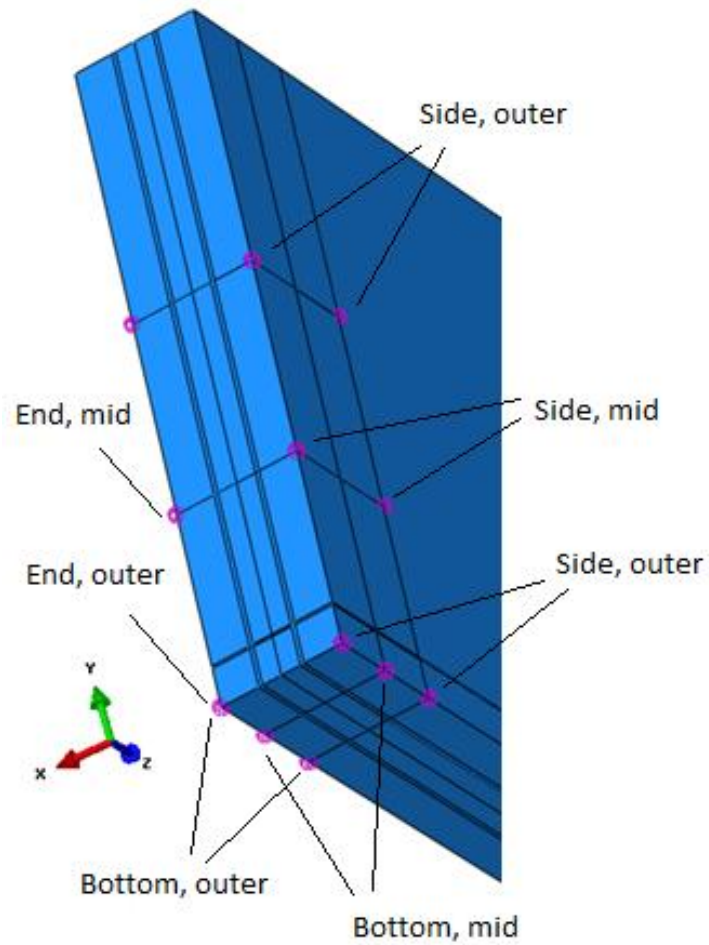


Figure 7.11: Boundary conditions for buckling analysis.

7.4 Results

7.4.1 Static analysis

Results from the static analysis of the beam are presented in Table 7.4.

	Stress glass (MPa)	Stress steel (MPa)	Strain interlayer	Deflection (mm)
Uncracked beam	32	90	3	3
Cracked beam	38	380	14	-

Table 7.4: Results from the static analysis of the beam.

7.4.2 Buckling analysis

The first eigenvalue was $1.52 \cdot 10^6$, thus the first buckling mode occurs at a distributed load of 1.52 MPa. The buckling mode shape can be seen in Figure 7.12.

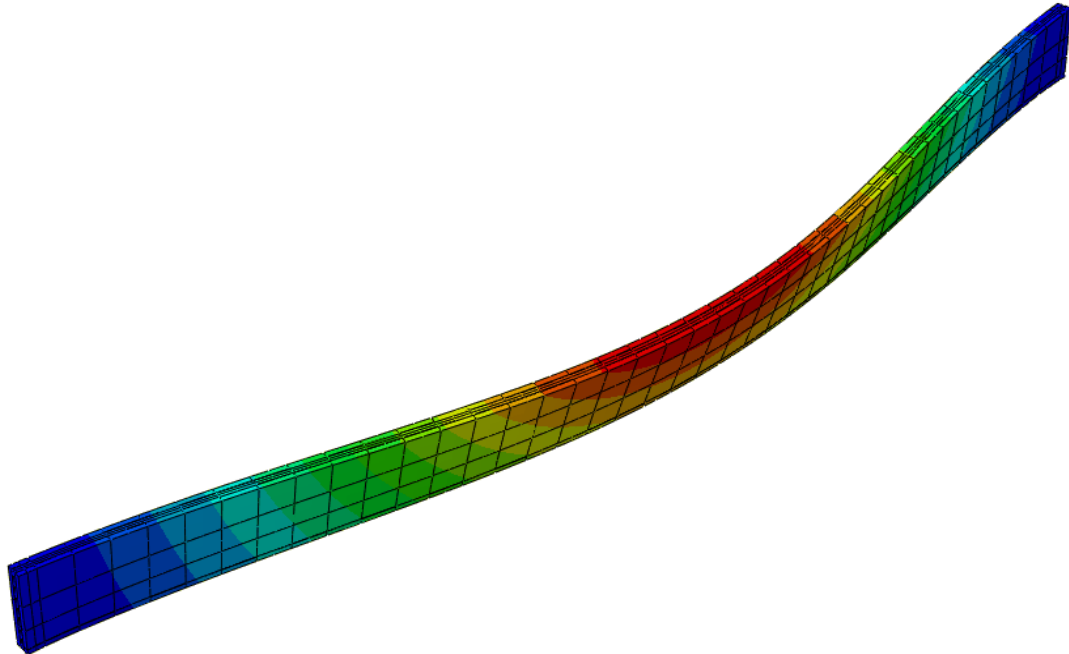


Figure 7.12: Buckling mode shape.

7.5 Modelling of beams presented from previous study

The beams tested by [5] were analysed to verify the results gained in this chapter considering the glass beams. Modelling of the beams was carried out in the same way as described in Section 7.2.

7.5.1 Description of the analysis

The beams were 1.6 meters long and consisted of two 6 mm thick glass layers on the sides and a 10 mm thick layer in the centre of the section, laminated together with two 1.52 mm thick layers of SGP. The beams were 125 mm high. A quadratic hollowed reinforcement made out of steel with dimension 10x10x1 mm acted in the bottom of the section. Dimensions of the beams can be seen in Figure 2.2.

The three different beams were of sort annealed glass, heat strengthened glass and fully tempered glass. The material data of the beams are shown in Table 7.5.

Property	Annealed glass	Heat strengthened glass	Fully tempered glass	Steel	SGP
Tensile strength [Pa]	45	70	120	520-750	34.5
Elastic modulus [N/mm ²]	70x10 ³	70x10 ³	70x10 ³	200x10 ³	300
Elongations at tear [%]	-	-	-	45	400
Density [kg/m ³]	2500	2500	2500	7900	950

Table 7.5: Material data of beams in the test study, [5].

The loading of the beams were carried out as four point loading, as can be seen in Figure 2.3. The loading leading to breakage carried out by [5] was 10.9 kN for the annealed glass beam, 33.1 kN for the heat strengthened glass beam, and 42.1 kN for the fully tempered glass beam. These were the loads that were applied during the analysis in Abaqus, along with a self weight of 0.3 MPa.

7.5.2 Results

The results from the analysis together with the characteristic values are presented in Table 7.6. The first column describes the characteristic tensile strength σ_{ct} (MPa), the stress values in the glass from the Abaqus modelling without cracks σ_{SA} (MPa) and the stress values in the steel reinforcement from the Abaqus modelling with cracks σ_{SAC} (MPa).

	Annealed glass	Heat strengthened glass	Tempered glass
σ_{ct} (MPa)	45	70	120
σ_{SA} (MPa)	42.4	129	164
σ_{SAC} (MPa)	460	458	400

Table 7.6: Results from analyses in Abaqus with input from previously performed test study, [5].

7.6 Conclusions

The intended beam met the requirements caused by the different types of loading. This as the stresses found in the glass were less than the design value of 43.1 MPa, and the deflection were less than $4000/300=13.3$ mm.

When cracking occurs, the steel must be able to carry a load of 380 MPa or more. The ferrit-austenitic steel: S32205 (EN 14462) [12] with a proof strength of 450 MPa and a tensile strength of 650-880 MPa, is chosen. The design strength value according to [13] is the same value as the characteristic value. It was also concluded that the number of cracks which occurs has negligible affects on the stresses in the beam and the difference in deflections between one and three sets of cracks were also negligible.

The buckling analysis gave the first instability at the load 1.52 MPa which was substantially higher than the applied load of 180.5 kPa. The beam will thus not break as a consequence of instability.

Concerning the previous carried out study it can be noticed that the stresses calculated in the Abaqus model were higher than the characteristic stresses considering heat-strengthened glass. This was expected since characteristic values are taken from the lower five percent fractile. Deviations from the characteristic values also depend on the glass used at the laboratory testing and on the strength of the glass. The actual bearing capacity of heat-strengthened glass is thus generally higher than 70 MPa. The stress value obtained in Abaqus concerning heat strengthened glass was 129 MPa when the failure load from the study was applied. Since the stress value obtained in the Abaqus model for heat-strengthened glass was a bit higher than the characteristic value, it is reasonable to conclude that the Abaqus model gives a good approximation of the actual glass beam.

The stress values in the annealed and tempered glass were also reasonably consistent with the characteristic values, with some deviations for the annealed glass which almost had the same stress in between the Abaqus model and the characteristic value. The stresses in the steel reinforcement were below the characteristic values of the material used. This is consistent with the laboratory testing since failure in the steel did not occur. These similarities between the Abaqus models and the laboratory testings concerning stress values in tempered glass, annealed glass and steel also implicates that the Abaqus model used is consistent.

8 Vibration analysis

Calculations concerning vibrations in the floor structure from dynamic loads acting on the system are performed in this chapter. The calculated vibrations were compared with guidelines given by [18].

8.1 Analysis of the system

8.1.1 Abaqus modelling

A combined structure consisting of beams and plates formed the model for the vibration analysis. It consisted of three beams and two rows of glass plates in between, as shown in Figure 8.1.

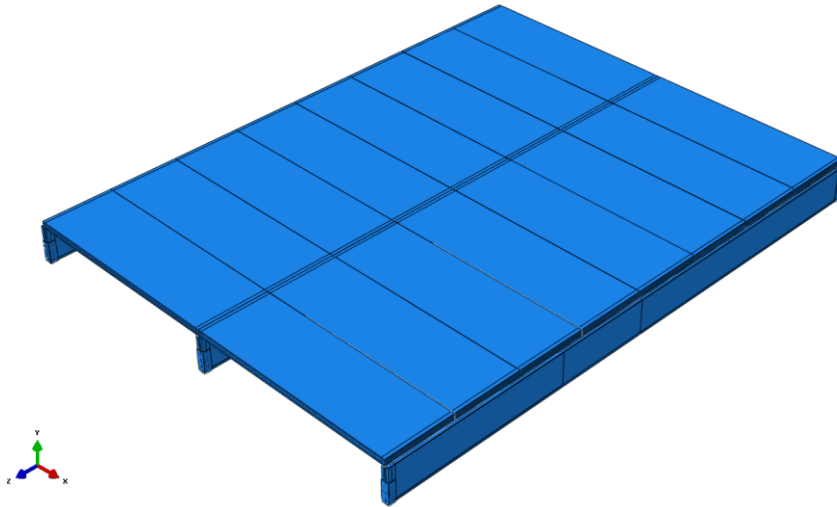


Figure 8.1: Model of the floor system used in the vibration analysis.

The boundaries between the plates and the beams consisted of silicone with rubber spacers. Since rubber and silicone have similar mechanical properties, all boundaries were assumed to be made of 3 mm thick rubber. At the edges of the beams layers of rubber material were assumed. These rubber layers had the purpose to form a soft boundary and to act as dampers. In Figure 8.2 such a boundary layer, mounted on a beam, is shown.

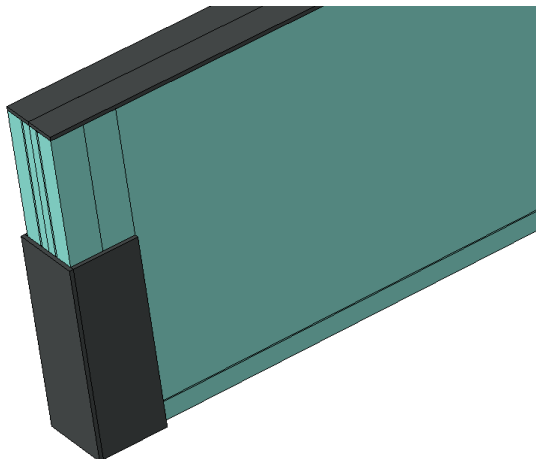


Figure 8.2: Rubber boundaries.

Damping parameters were introduced as material damping for the rubber and the SGP layers. Rayleigh damping was employed in this modelling and the two damping coefficients a_0 and a_1 were calculated with eq. (4.21) using the frequencies 1 Hz and 10 Hz. Both frequencies were assumed to have the same damping ratio, which was 7 %. A commonly used standard value for damping in building codes is 5 %. Recommended damping values can vary between about 2-20 % though, where steel normally has a damping ratio of 5 % and wood 15 %, just below the yield point [15]. These damping ratios can be used directly for the linearly elastic analysis of structures with classical damping [15]. The rubber was assumed to have a damping ratio of 7 %, which should be on the safe side concerning propagation of vibrations.

Two different steady state vibration analyses were performed. The first analysis was to verify the response of the structure concerning vibrations acting vertically on the floor, and the second analysis was to verify the response of the structure concerning vibrations acting laterally on the floor.

8.1.2 Evaluation of vibrations

The allowed maximum values concerning vibrations at different sites are shown in Figure 8.3 [18].

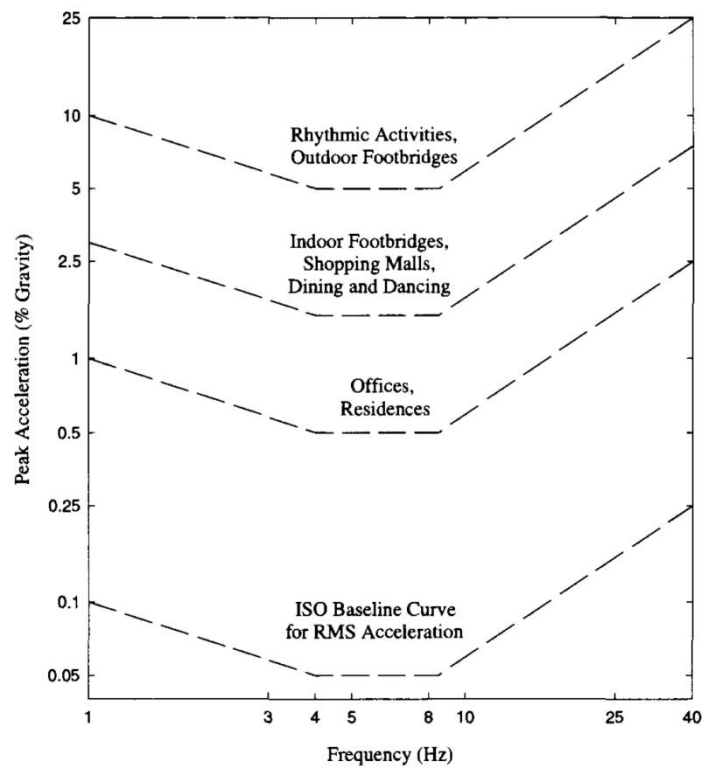


Figure 8.3: Maximum values concerning vibrations at different sites, [18].

The load acting on the structure will mainly come from people walking on the floor and the vibrations caused by their footsteps. The load acting in the vertical direction was decided to be 1 N in total, which was spread out over the total floor area of 12 m². A load of 1 N was applied since the relation between the load and the accelerations is linear, which allows loading from the people to be varied after the accelerations from the steady state analysis were calculated. The total load of 1 N resulted in a uniformly distributed load of 0.083 N/m². Concerning vibrations in the vertical direction, 12

persons were assumed to be walking on the floor at the same time. The position of the largest vertical accelerations is shown with a red circle in Figure 8.4. These accelerations were compared to the allowed maximum acceleration values.

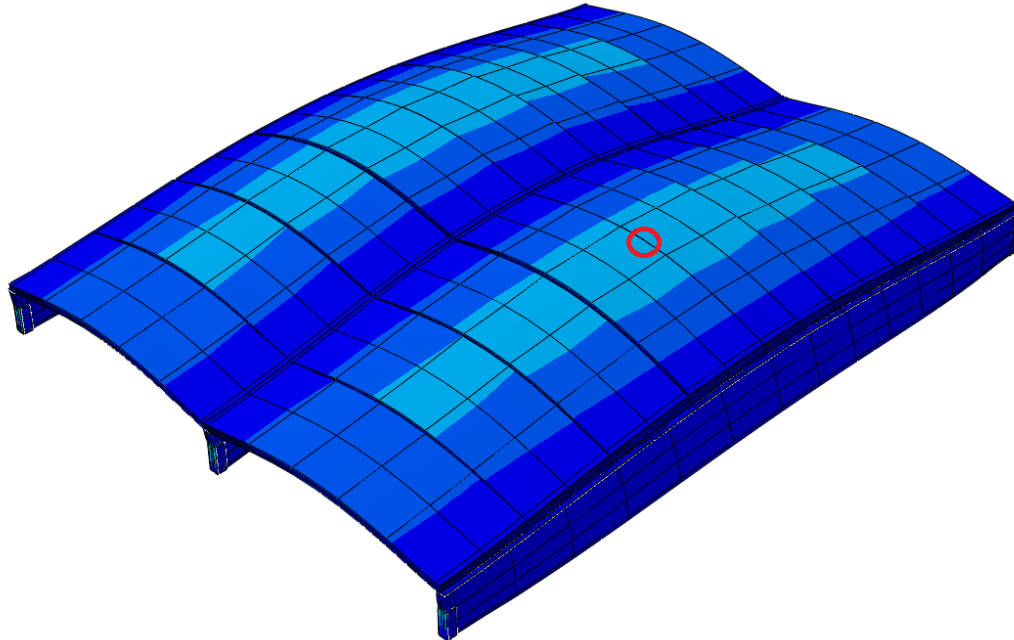


Figure 8.4: Largest vertical accelerations.

In the analysis concerning the lateral vibrations 3 people was assumed to act as concentrated loads, as shown in Figure 8.5. The total load acting in the lateral direction was decided to be 1 N for the same reasons as described for the vertical vibrations. This resulted in three forces of 0.33 N each. The largest accelerations were those at the tip of the mid arrow in Figure 8.5. These accelerations were compared to the allowed maximum acceleration values.

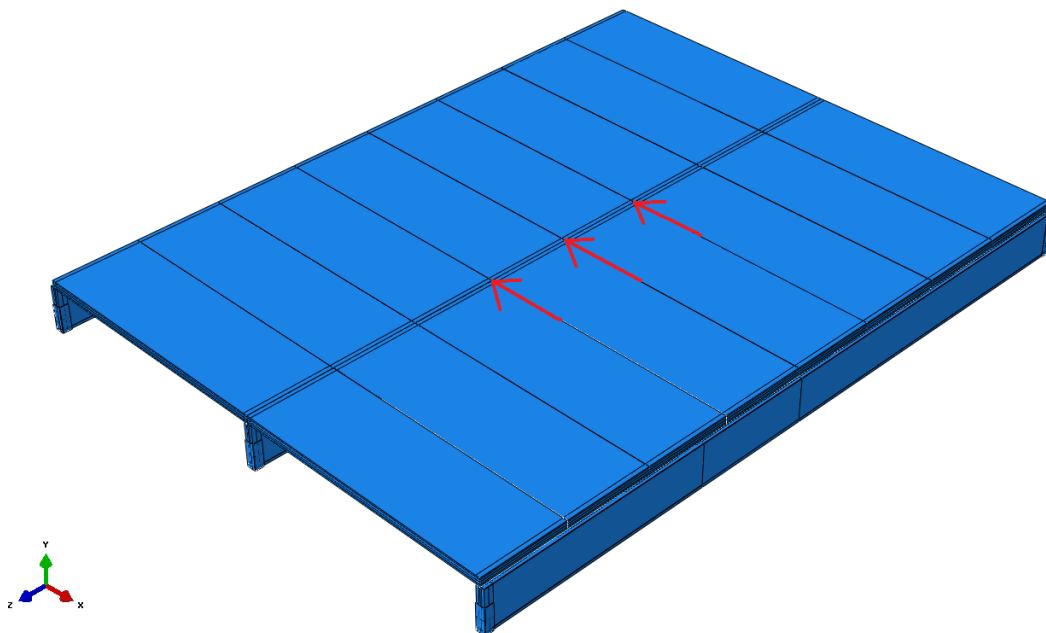


Figure 8.5: 3 Lateral point loads.

The mass of the people was added to the mass density of the beams during the analysis. The accelerations of the structure when excited by dynamic forces with frequencies between 1-10 Hz were inserted into a MATLAB program. In this program the amount of people moving on the floor could be decided and the vibrations could be calculated and plotted.

8.2 Results

8.2.1 Damping coefficients

By solving eq. (4.21) with the frequencies 1 Hz and 10 Hz combined with a damping ratio of 7 %, the Rayleigh damping coefficients were calculated to $a_0=0.8$ and $a_1=0.002$.

8.2.2 Vibrations

The accelerations of the system related to the acceleration of gravity were obtained with eq. (5.4). The results concerning the vertical vibrations of the structure can be seen in Figure 8.6 and the results concerning lateral vibrations of the structure can be seen in Figure 8.7. The accelerations were compared with two curves. The pink line in Figure 8.6 is the baseline curve and the black line is the limit for offices and residences [18]. The pink line in Figure 8.7 is the baseline curve [18]. Vibrations under the baseline curve represent vibrations that cannot be felt by a human being. The red lines in Figure 8.6 and Figure 8.7 represent the system's actual accelerations, without the reduction coefficients found in Table 5.2.

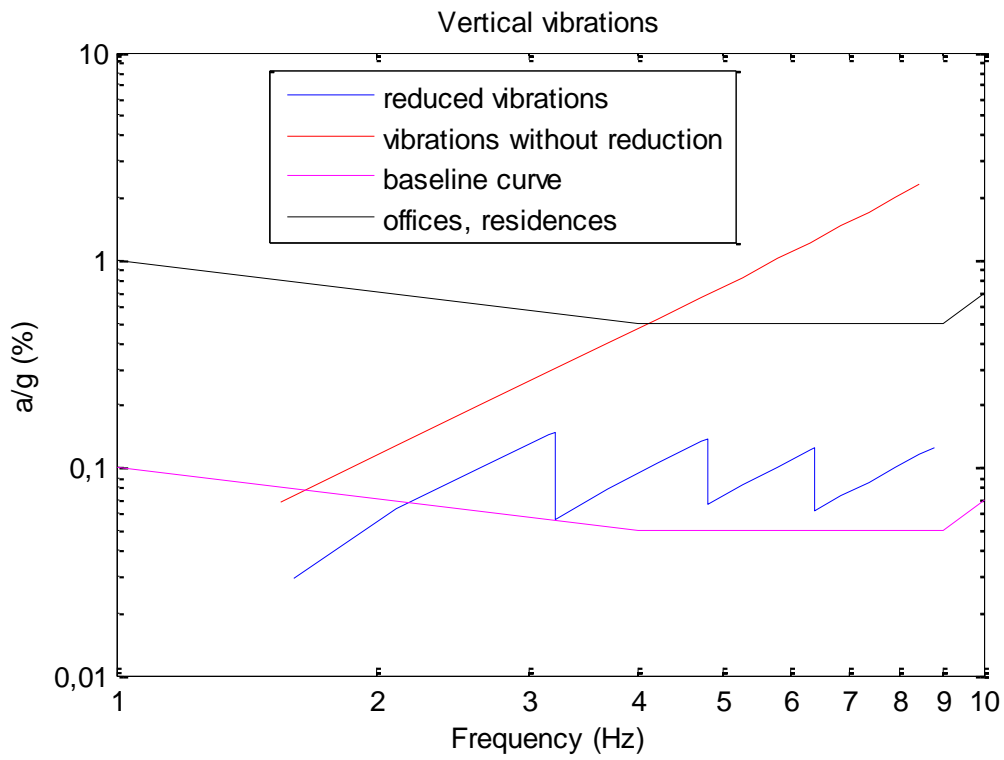


Figure 8.6: Vertical vibrations of the glass system.

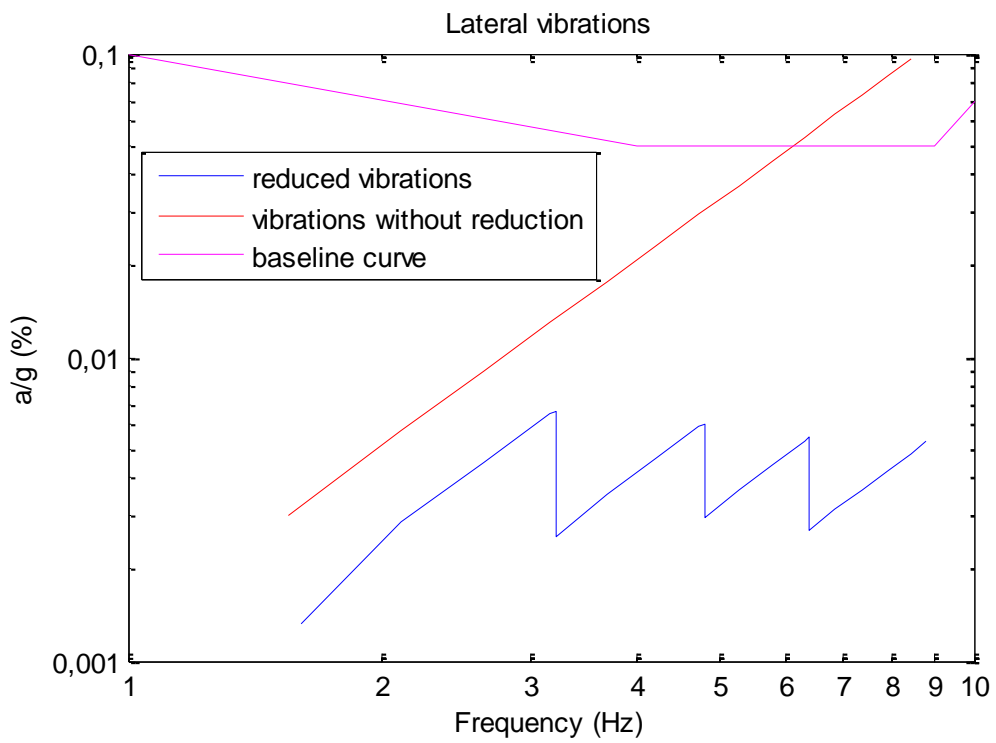


Figure 8.7: Lateral vibrations of the glass system.

8.3 Conclusions of the vibration analysis

For a glass floor in a public place the vibrations should not exceed the line which corresponds to Indoor Footbridges, Shopping Malls and Dining and Dancing; as shown in, Figure 8.3. The vertical vibrations obtained from the analysis were not only below this limit but also below the limit corresponding to Offices and Residences in Figure 8.3. The lateral vibrations had values that were even lower than the vertical vibrations. A conclusion that can be made from the vibration analyses is that the glass system will be well under the limit for both vertical and lateral vibrations given by [18]. However the analysis was performed with some assumptions that may affect the results.

One assumption was the damping ratios used for the rubber and interlayers. Damping ratios vary between different structures and it is hard to obtain the correct value without performing tests on the actual structure. Since the structure discussed in this report has not been erected, experimental testing was not possible. The damping ratios affect the vibrations and with different assumptions of damping ratios, different results will be obtained. Also the damping ratio of the glass was neglected which could have a minor affect on the results. Another assumption when performing the analysis was the amount of people walking on the floor. One person per square metre was assumed for the vertical vibrations and three people acting as concentrated loads were assumed for the lateral vibrations. These values could be both higher and lower than the assumed values and thus have an impact on the results.

At the ends of the beams, rubber boundaries were placed which can be seen in Figure 8.5. The glass is not fastened in these rubber boundaries but is held in place by friction. In the case of dynamic loading this friction connection will allow the glass to slide small distances relative to the rubber. However, in the vibration analyses the glass was fastened all along the rubber boundaries which created a stiffer connection than intended in reality. If the glass would be allowed to move small distances in the rubber boundaries, it could result in slightly larger vibrations in the model.

It can be concluded from the red lines in Figure 8.6 and Figure 8.7 that the system did not have any natural frequencies between 1-10 Hz. If a natural frequency would exist in this frequency interval the system would exhibit resonance and the red line would have had a peak. The lack of a natural frequency in or close to the interval 1-10 Hz is another reason to that the accelerations were small.

9 Design of the whole system involving boundaries

This chapter describes the system with dimensions for the complete floor structure. Parts that have been described in earlier chapters are here shown added together with figures. The purpose of this chapter is to give an understanding of the system and the connections. The conclusions made concerning sizes of different sections in earlier chapters are put together and the whole system is shown. Practical issues are discussed and suggestions concerning a wear layer and erection method are presented.

9.1 Description of the system with dimensions

As verified in previous chapters, a single glass plate has a dimension of 1.5x0.5 m, with a thickness of 8-12-12-8 mm glass, with 3x1.52 mm polymer interlayer in between. The beams are 4 m long and 250 mm high. The cross section of the beams consists of 3x15 mm heat strengthened glass plates with 2x1.52 mm SGP interlayer in between. A quadratic profile of steel with dimension 15x15 mm² runs along the bottom of the centric glass plate, laminated together with the rest of the glass beam. The steel is of type: S32205 (EN 14462).

The beams are simply supported on U-shaped boundaries at the ends. The boundaries are connected to steel columns, for example VKR-40x40-2.5. However a closer calculation of the columns has to be performed in order to verify the exact dimension. At the location where two beams meet each other on a column there is a layer of rubber to prevent the beams to interfere with each other. A basic detail of the section can be seen in Figure 9.1.

The glass plates are glued to the beams using a silicon adhesive with rubber spacers in between. In the connection between all the glass plates will be a soft silicon adhesive.

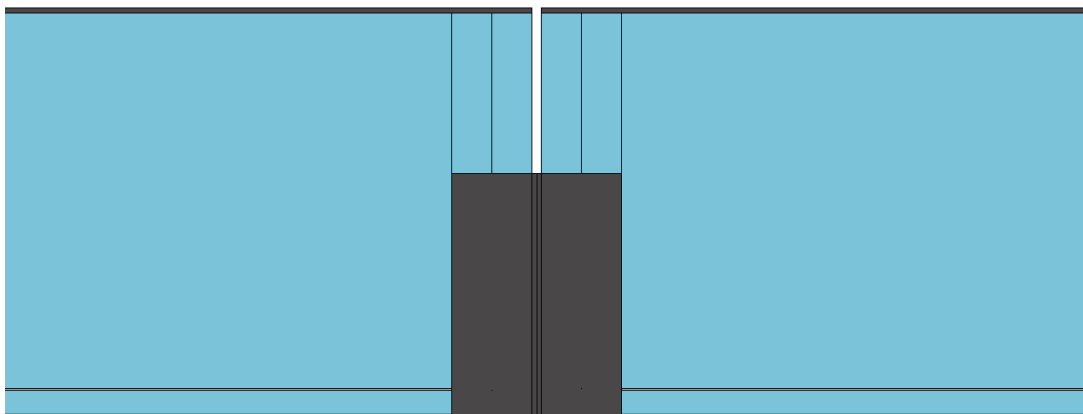


Figure 9.1: Basic detail of connection between two beams.

A glass with a low content of iron will provide the best results in the intended glass structure, since iron colours glass and give it a tone of green that can be undesirable

especially for thicker profiles. The green tone in normal glass gets stronger with an increased thickness and will therefore probably dominate the appearance of the structure.

9.2 Wear layer

On top of the glass plates a surface wear layer must be employed. This is to prevent scratching of the glass plates and to allow impacts to some extent. Scratching is not desirable as it can affect the durability of the structural strength of the glass plates. In the case that the surface is exposed to a severe impact, a wear layer can be useful as it can take the main concentrated part of the impact and smear it out to the other plates. If a wear layer cracks it is rather easy and cheap to replace, whereas a replacement of an entire glass plate is much more expensive. The surface wear layer will be a single glass layer attached on top of the glass plates. It can be desirable to make the layer thin since a thinner layer is easier to replace.

9.3 Attachments

The beams will be simply supported on U-shaped boundaries at the ends covered with rubber. The boundary between the glass beams and the glass plates will consist of silicone with rubber spacers. Between each glass plate, silicon is used as the adhesive. No screws or bolts will be necessary at the ends of the beams, friction between the rubber and the glass will keep the structure in place.

9.4 Erection of the system

When the system is to be erected, the columns are first put in place. The next step is to install joist hangers at top of the columns. These will be clad in rubber as shown in Figure 7.9. The beams will then be lifted into place on the rubber boundaries and will hence be simply supported. After the beams are put in place the glass plates are to be installed. The glass plates will be put on the rubber spacers on top of the beams and glued to the beams using silicone. Silicone will also be used between each plate along the beams. All the plates are to be simply supported just as the beams. Finally when all the structural elements are in place the wear layer can be installed on top of the system. Actions concerning safety against fire are discussed in Chapter 10. The glass system containing glass plates, beams and rubber boundaries is shown in Figure 9.2 and Figure 9.3.

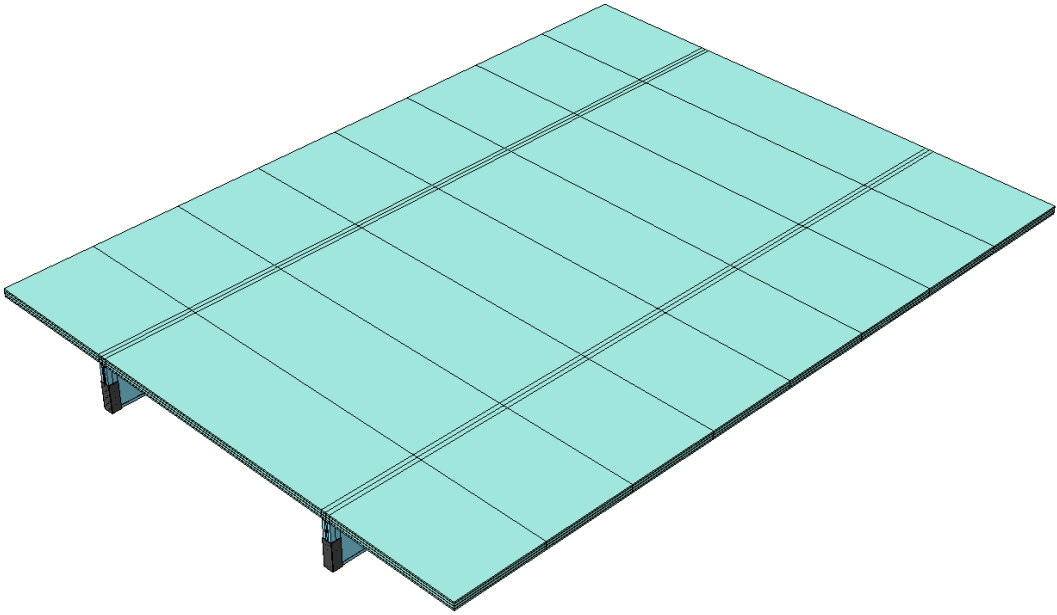


Figure 9.2: Section of the glass floor, seen from above.

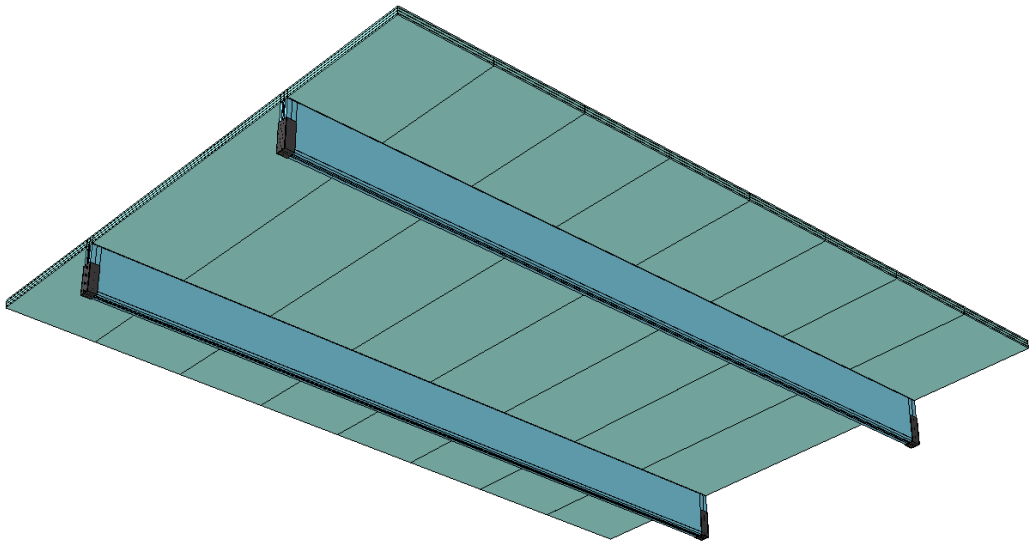


Figure 9.3: Section of the glass floor, seen from below.

10 Design concerning resistance against fire

This chapter is dealing with fire and what a fire development looks like. Fire resistance of the system and its ability to withstand a fully developed fire is here taken into account. Actions to reduce a fire development are hence introduced.

10.1 Fire progression

A fire normally includes two important phases; initial fire and fully developed fire. After this phases, a cooling phase follows. The temperature increase of a fire is rather rapid and a few minutes are all that is needed for it to fully develop.

A fire in a building usually starts in the decor, for example in furniture or curtains. This is often a result of carelessness with candles, cigarettes and the like [28]. During a fire a smoke cloud rises towards the ceiling and a hot layer of fire gases forms. This is followed by a quickly raising temperature which can lead to a flashover. A flashover is when all the combustible materials and surfaces in the room catch fire, the cloud of fire gases will drop towards the floor and flames will appear in the smoke cloud. The temperature when this happens is about 500-600°C and swiftly increasing during this stage [28].

A flashover is followed by a fully developed fire, which can last for a few minutes up to a few hours, depending on the supply of fuel and oxygen. The radiation levels towards the floor will be about 15-20 kW/m² during this stage, which is more than a human being can endure [28]. How the fire develops in case of temperature and intensity is decided by how much oxygen the fire has access to, how much material that is available as fuel, and the ignition temperature of these. The cooling phase begins when the fuel in the room runs out. The temperature and intensity of the fire will then decrease over a period of one to a few hours [28].

10.2 Fire safety requirements

The Construction Products Regulation (CPR) contains seven essential requirements for safety in buildings. One of these requirements concerns fire safety [27]. According to this requirement a building shall be designed and built so that the following is achieved in the case of a fire [27]:

- The construction's bearing capacity is assumed to be intact during a determined time.
- Development and spread of fire and smoke within the construction are limited.
- Spreading of fire to neighbouring constructions is limited.
- People who are in the construction can leave it or be saved in some other way.
- Safety of rescue teams is considered.

What the above mentioned statements mean for the glass structure discussed in this report is that the glass floor must be able to still carry load for a determined time during a fire. People that are on the floor must at the same time be able to evacuate, and the safety of the rescue team which will put out the fire, must be considered.

10.3 Fire resistance of glass

In order to construct a glass system that meets the requirements of fire safety it is natural to look at other materials and how to make them fire resistant. Glass and steel are normally considered bad materials considering fire safety, but fire resistant buildings are constructed using steel as the load bearing material. To create fire safe buildings in steel, the material can be cast into concrete or painted with a fire resistant coating. These solutions protect the steel against too rapid a rise in temperature [8], which gives the people in the building more time to evacuate. However these solutions cannot be applied on glass since it is a transparent material and insulation or paint would ruin the appearance and hence disregard the main reason to use glass as construction material.

The National Research Council of Canada (NRCC) have done tests concerning the effect of fire on annealed glass, heat strengthened glass and tempered glass [29]. When the annealed glass was exposed to high radiation it broke within minutes with a temperature on the exposed side of 150-175°C.

The heat strengthened glass and tempered glass did not crack until the temperature reached 350°C [29]. The radiation level used was 10 and 40 kW/m² for plain glass and 43 kW/m² for heat strengthened glass and tempered glass.

The test carried out by NRCC also included a study where sprinklers were used to verify which effect the thermal shock of water spray had on the glass. The results from these tests were that the annealed glass could withstand the impact of water spray at 80-90°C, the heat strengthened glass at 150-165°C and tempered glass at 200°C [29]. If the glass specimens had a higher temperature than this, the glass would crack when water spray reached the surface.

The tests carried out by the NRCC showed that the worst case scenario when using sprinklers to put out a fire was when a small fire developed close to the glass. In this scenario standard sprinklers were not efficient in protecting the glass, only fast response sprinklers located close to the glass would activate early enough to protect the glass from cracking [29].

10.4 Fire resistance of polymers

Normally polymers are not designed to work in extreme temperatures and will melt or burn when a high temperature is reached in the material. The SGP interlayer has a melting point at 94°C [30]. When this temperature is reached its ability to act as an interlayer is considerably decreased. EPDM rubber will lose its properties after 100°C [9] and will start to burn at about 300°C. Silicone is normally heat resistant until about 200°C is reached [11].

10.5 Simulation of fire

A simplified simulation of a fire with an ISO 834 standard heating curve in the software Argos was carried out. The surface temperature development in the glass profile was calculated and plotted by the program with the assumption that the worst case scenario is when a fire affects the glass beam on both sides. The analysis was

performed and plotted until the transition point of glass was reached, which is about 600°C [1]. Figure 10.1 shows the temperature distribution through the glass beam during a fire without any measures on site to decrease the influence of the fire. Figure 10.2 shows the surface temperature only, of the same beam.

As can be seen in Figure 10.1 and Figure 10.2 a temperature of 150°C is reached after about 90-120 seconds at the surface of the beam. The temperature 15 mm into the beam at the laminate layer between the outer and the inner glass plates, has reached a temperature of 100°C after about 400 seconds. The temperature at the surface will at the same time be about 400°C.

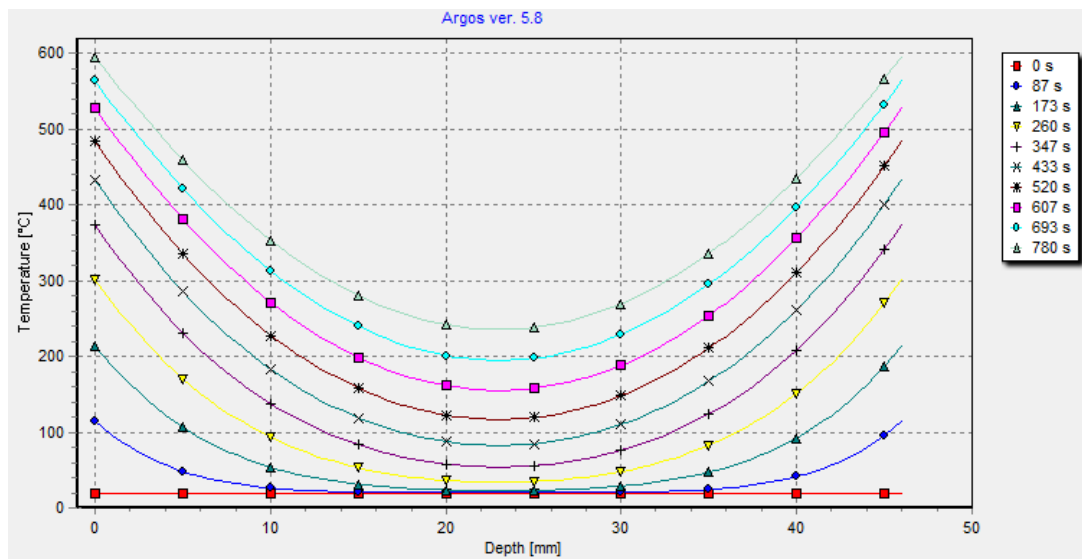


Figure 10.1: Temperature in a cross section of a glass beam exposed to fire, plotted against time.

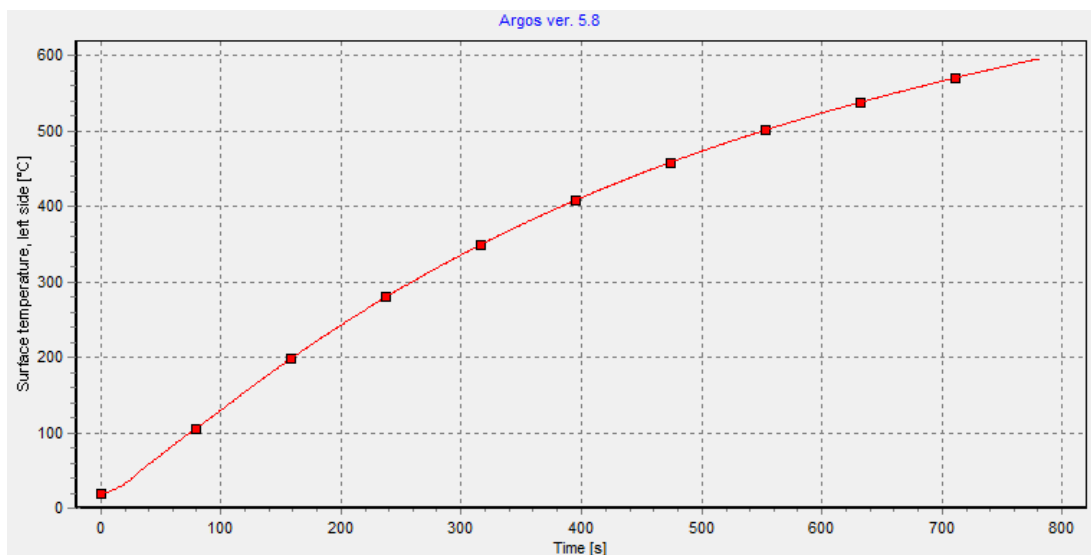


Figure 10.2: Surface temperature off a glass beam exposed to fire, plotted against time.

At the beginning of a fire the floor consisting of glass plates will most likely only be affected by the fire on one side of the floor. As shown in Chapter 6, three glass plates will be enough to carry the load acting on the plates in a worst case scenario. This means that the durability of the glass plates probably will be longer than the durability of the beams. On the other hand, if fire affects the plates on both sides the durability time will reduce and hence reach a value below the one calculated for a beam.

10.6 Conclusion

Heat strengthened glass can withstand temperatures of 150-165°C without cracking when sprayed with water from a sprinkler system. However the interlayers can only withstand temperatures of around 100°C. To reach a temperature of 150°C on the surface, will take about 90-120 seconds in a normal fire development, and to reach a temperature of 100°C in the outermost interlayer will take about 400 seconds. The temperature will thereby reach a critical level in the glass at the surface before it reaches a critical level in the interlayer.

In order to prevent the structure from collapsing, the sprinkler system must be activated 90 seconds after the fire starts and there must be sprinklers to spread water above and underneath the floor. If a fire concentrated to a small area close to the glass structure were to occur, only fast response sprinklers close to the glass structure would be able to activate early enough to protect the glass [29]; however placing sprinklers close to the glass floor can be problematic from an aesthetical and practical point of view.

Another solution is to put the sprinklers underneath the glass floor and further away on top of the floor. This would ensure an efficient sprinkler system close to the glass at least considering the beams. This solution would protect the glass beams fully and the plates from underneath. On the other hand, if the upper plate starts to crack due to a slow acting sprinkler system, this would not be catastrophic, as the floor can carry the load with less than four plates.

Ensuring that a bearing glass structure is fully resistant against fire is a hard task and is not handled in this report. In order to ensure a fireproof glass structure the temperature of the glass must be limited in some way, one possible solution is the previously discussed one using sprinklers, but for this kind of structure the sprinkler system must be very reliable and well built.

11 Final remarks

In this chapter the authors give a final conclusion considering the results in the report and give some suggestions for further work.

11.1 Conclusions

Out of the results gained in this report the authors conclude that the glass system presented will be able to carry the required loads concerning a congregation area given by Eurocode. The system can handle the loads given without reaching critical stress levels or too large deflections in the profiles, even when cracks are introduced. The results also showed that no instability considering buckling will occur and that the vibration levels in the system will be well below the limit presented in guidelines. Considering fire resistance of the structure it is clear that further investigations must be carried out. The investigations presented in this report however, showed that fire is a critical factor that will be a hard task to solve, bearing in mind that the transparent properties of the system must be preserved.

11.2 Further studies

The results presented in this report came from Abaqus models and no laboratory testing has been done. To establish that the system works as intended by the models, laboratory testing has to be conducted. A suggestion for further work is therefore to construct the glass system presented in this report and to measure stresses, deformations, instability and vibrations at site. In laboratory testing of the glass system more accurate damping values can be found, which would enable a computer model to present more accurate results.

Another suggestion for further work is to perform laboratory testing on the rubber boundaries. These tests should be focused on the adhesion between the glass plates and the glass beams, and the friction connection between the end of a beam and its rubber boundary. This study would conclude if these boundaries would behave as intended by the computer models.

The size and placement of the cracks in the system were based on a previous study [5] and approximations made by the authors. The stresses in the system were critical when cracks were present and since the size and placement of the cracks were somewhat approximated, the dimensions of the glass plates and glass beams was also approximated. In order to better optimize the use of material in the structure a more extensive analysis would have to be carried out on the cracks in the system.

One big issue when constructing glass systems is to make them able to manage safety requirements during a fire. Only a brief introduction to the effects of fire on glass and a few suggestions on how to make a glass system safe against fire were given in this report. To be able to build glass systems, solutions that ensure a glass system's safety during a fire have to be developed and tested. Another suggestion for further work is thus to find out how to improve the fire resistance of glass and how to construct a system that can manage the various requirements given for a fire-proof structure.

12 Bibliography

- [1] Flygt, Elisabeth et al. (2004), *Boken om glas*, Glafo
- [2] Capital Glass. *What is the difference between Annealed, Heat Strengthened, and Tempered Glass?*, Capital Glass, Inc.
<http://www.capitalglassonline.com/FAQRetrieve.aspx?ID=39330>, visited 2014-02-25
- [3] Belis, Jan et al. (2012). *Experimental Investigation of Unconventional Canopy Prototypes, Suspended by Adhesive Bonds*, Challenging Glass 3 – Conference on Architectural and Structural Applications of Glass
- [4] Forserum Safety Glass AB. *Värmeförstärkt glas*, Forserum Safety Glass AB.
<http://www.fsglass.se/Svenska/Produkter/V%C3%A4rme%C3%B6rst%C3%A4rktglas.aspx>, visited 2014-02-25
- [5] Louter, Christian et al. (2012). *Reinforced Glass Beams Composed of Annealed, Heat- Strengthened and Fully Tempered Glass*, Challenging Glass 3 – Conference on Architectural and Structural Applications of Glass
- [6] Terselius, Björn (2013). *Polymer*, Nationalencyklopedin,
<http://www.ne.se/lang/polymer>, visited 2014-02-25
- [7] SGP (2008), *SGP® Plus Elastic Properties (SGP 5000)*, DuPont
- [8] Burström, Per Gunnar (2003). *Byggnadsmaterial*, Studentlitteratur
- [9] Trelleborg (2005). *TEKNISK SPECIFIKATION MATERIAL: 7001 EPDM*, Trelleborg AB,
http://www.trelleborg.com/upload/Elastomer%20Laminates/Swedish%20version/pdf/Teknspec_7001.pdf, visited 2014-02-25
- [10] Terselius, Björn (2013). *Lim*, Nationalencyklopedin,
<http://www.ne.se/lang/lim/241669>, visited 2014-02-25
- [11] MASTERBOND (2013). *MasterSil 702 Product Description*, Master Bond inc.
<http://www.masterbond.com/tds/mastersil-702>, visited 2014-02-25
- [12] Bröderna Edstrand [1999]. *Röda katalogen: Teknisk handbook*, Bröderna Edstrand AB
- [13] Isaksson, Mårtensson (2010). *Byggkonstruktion*, Studentlitteratur
- [14] Ottosen, Petersson (1992). *Introduction to the Finite Element Method*, Prentice Hall
- [15] Chopra, Anill K. (1995). *DYNAMICS OF STRUCTURES*, Prentice Hall

- [16] Kursmaterial. (2013). Strukturdynamiska beräkningar, VSMN10, Faculty of Engineering at Lund University
- [17] Delincé, Didier et al. (2008). *Post-breakage behaviour of laminated glass in structural applications*, Challenging Glass – Conference on Architectural and Structural Applications of Glass
- [18] Murray, Allen, Ungar (2003). *Floor Vibrations Due to Human Activity*, American institute of steel Construction Inc.
- [19] Dassault Systèmes SIMULIA (2013). *Abaqus 6.11 Documentation*, Daussault Systèmes Inc S.A, <http://abaqus.ethz.ch:2080/v6.11/>, visited 2014-02-25
- [20] European Standard (2013). *Glass in building- Determination of the load resistance of glass panes by calculation and testing*, Technical Committee CEN/TC 129
- [21] Kursmaterial. (2012). *BALKTEORI*, KFS AB
- [22] SGP, *SGP® Plus vs. PVB for laminated Glass*, DuPont. http://www2.dupont.com/Building_Innovations/zh_CN/assets/downloads/SGPintro_E.pdf, visited 2014-02-25
- [23] Le Bourhis, Eric (2007). *Glass*, WILEY-VCH
- [24] Lindley, P. B. (1978). *Engineering design with natural rubber*, Hertford Offset Ltd
- [25] Krenk, Steen [2009]. *Non-linear Modelling and Analysis of Solids and Structures*, Cambridge University Press
- [26] Ottosen, Ristinmaa (2005). *The Mechanics of Constitutive Modelling*, Elsevier Ltd
- [27] Europaparlamentet och Rådets Förordningar [2011]. *Byggproduktförordningen (CPR) 305/2011*, Official Journal of the European Union
- [28] Svensk Trä [2014]. *TrägGuiden*, Svenskt Trä. <http://www.traguiden.se/TGtemplates/GeneralPage.aspx?id=8046>, visited 2014-02-25
- [29] Kim, Loughheed [1990]. *Journal of Fire Protection Engineering*, SAGE
- [30] SGP, *SGP® Brochure*, DuPont. http://www2.dupont.com/SafetyGlass/en_US/assets/pdfs/SGP_brochure.pdf, visited 2014-02-25
- [31] Carlsson, Janne (2014). *Brottmekanik*, Nationalencyklopedin, <http://www.ne.se/lang/brottmekanik>, visited 2014-02-19